

Metabolism of Vertebrate Amino Sugars with *N*-Glycolyl Groups

ELUCIDATING THE INTRACELLULAR FATE OF THE NON-HUMAN SIALIC ACID *N*-GLYCOLYLNEURAMINIC ACID^{*†}

Received for publication, March 22, 2012, and in revised form, May 25, 2012. Published, JBC Papers in Press, June 12, 2012, DOI 10.1074/jbc.M112.363549

Anne K. Bergfeld, Oliver M. T. Pearce, Sandra L. Diaz, Tho Pham¹, and Ajit Varki²

From the Departments of Medicine and Cellular and Molecular Medicine, Glycobiology Research and Training Center, University of California San Diego, La Jolla, California 92093-0687

Background: Pathways for turnover and degradation of the mammalian sialic acid *N*-glycolylneuraminic acid (Neu5Gc) are currently unknown.

Results: Mammalian cells can degrade Neu5Gc by sequential conversion into *N*-glycolylmannosamine, *N*-glycolylglucosamine, and *N*-glycolylglucosamine 6-phosphate, following release of glycolate and glucosamine 6-phosphate.

Conclusion: Basic *N*-acetylhexosamine pathways seem tolerant toward the *N*-glycolyl substituent.

Significance: We elucidate the metabolic turnover of the diet-derived human xeno-autoantigen Neu5Gc.

The two major mammalian sialic acids are *N*-acetylneuraminic acid and *N*-glycolylneuraminic acid (Neu5Gc). The only known biosynthetic pathway generating Neu5Gc is the conversion of CMP-*N*-acetylneuraminic acid into CMP-Neu5Gc, which is catalyzed by the CMP-Neu5Ac hydroxylase enzyme. Given the irreversible nature of this reaction, there must be pathways for elimination or degradation of Neu5Gc, which would allow animal cells to adjust Neu5Gc levels to their needs. Although humans are incapable of synthesizing Neu5Gc due to an inactivated *CMAH* gene, exogenous Neu5Gc from dietary sources can be metabolically incorporated into tissues in the face of an anti-Neu5Gc antibody response. However, the metabolic turnover of Neu5Gc, which apparently prevents human cells from continued accumulation of this immunoreactive sialic acid, has not yet been elucidated. In this study, we show that pre-loaded Neu5Gc is eliminated from human cells over time, and we propose a conceivable Neu5Gc-degrading pathway based on the well studied metabolism of *N*-acetylhexosamines. We demonstrate that murine tissue cytosolic extracts harbor the enzymatic machinery to sequentially convert Neu5Gc into *N*-glycolylmannosamine, *N*-glycolylglucosamine, and *N*-glycolylglucosamine 6-phosphate, whereupon irreversible de-*N*-glycolylation of the latter results in the ubiquitous metabolites glycolate and glucosamine 6-phosphate. We substantiate this finding by demonstrating activity of recombi-

nant human enzymes *in vitro* and by studying the fate of radio-labeled pathway intermediates in cultured human cells, suggesting that this pathway likely occurs *in vivo*. Finally, we demonstrate that the proposed degradative pathway is partially reversible, showing that *N*-glycolylmannosamine and *N*-glycolylglucosamine (but not glycolate) can serve as precursors for biosynthesis of endogenous Neu5Gc.

Mammalian cells typically decorate their surfaces with a variety of glycoconjugates, and the terminal position of their glycan chains is commonly occupied by sialic acids (1–4). Among the >50 naturally occurring sialic acid derivatives, mammalian cells predominantly synthesize and express *N*-acetylneuraminic acid (Neu5Ac)³ and *N*-glycolylneuraminic acid (Neu5Gc). Activation of sialic acids occurs in the nucleus, and the resulting CMP-activated sialic acids are transported to the Golgi apparatus, where they are transferred onto underlying glycan chains by action of >20 sialyltransferases (5). The only known biosynthetic pathway yielding Neu5Gc takes place at the level of activated sugars and results in conversion of CMP-Neu5Ac into CMP-Neu5Gc, which is catalyzed by the cytosolic CMP-Neu5Ac hydroxylase (*CMAH*) (6–13). In humans, the single copy *CMAH* gene was found inactivated (14, 15) by an *Alu*-mediated replacement of a 92-bp exon resulting in a frameshift mutation (14, 16, 17). The complete absence of Neu5Gc in *Cmah*^{-/-} mice carrying the human-like mutation (18) suggests that humans completely lost the ability for *de novo* Neu5Gc biosynthesis. Despite the lack of an alternative pathway for Neu5Gc synthesis, the presence of Neu5Gc has been conclusively demonstrated on various human carcinomas and in fetal

* This work was supported, in whole or in part, by National Institutes of Health Grants R01GM32373 and R01CA38701 (to A. V.). This work was also supported by Deutsche Forschungsgemeinschaft Research Fellowship BE 4643/1-1 (to A. K. B.) and a Cancer Research Institute/Samuel and Ruth Engelberg Fellowship (to O. M. T. P.). A. V. is a co-founder of and consultant for Sialix Inc., a biotech startup company interested in the practical implications of Neu5Gc uptake in humans.

† This article contains supplemental Figs. S1–S5.

¹ Present address: Stanford School of Medicine, Dept. of Pathology, 300 Pasteur Dr., Stanford, CA 94304.

² To whom correspondence should be addressed: Glycobiology Research and Training Center, Depts. of Medicine and Cellular and Molecular Medicine, University of California San Diego, 9500 Gilman Dr., University of California San Diego, La Jolla, CA 92093-0687. Tel.: 858-534-2214; Fax: 858-534-5611; E-mail: a1varki@ucsd.edu.

³ The abbreviations used are: Neu5Ac, *N*-acetylneuraminic acid; Neu5Gc, *N*-glycolylneuraminic acid; *CMAH*, CMP-Neu5Ac hydroxylase; CV, column volume; DMB, 1,2-diamino-4,5-methylenedioxybenzene; GlcNGc, *N*-glycolylglucosamine; HPAEC-PAD, high performance anion exchange chromatography-pulsed amperometric detection; ManNAc, *N*-acetylmannosamine; ManNGc, *N*-glycolylmannosamine; P, phosphate; EDC, ethyl-3-(3-dimethylaminopropyl)-carbodiimide; sulfo-NHS, *N*-hydroxysulfosuccinimide; Sia, sialic acid.

Metabolic Fate of N-Glycolylneuraminic Acid

meconium (19–24). With the development of additional sensitive detection methods, low levels of Neu5Gc have been found on normal human tissues such as endothelia of blood vessels (25, 26) and apparently originate from Neu5Gc-rich dietary sources such as red meats (26, 27). Our companion paper (28) shows for the first time that *Cmah*^{-/-} mice incorporate dietary Neu5Gc with a human-like bodily distribution after feeding with Neu5Gc-containing glycoconjugates. Indeed, human cells were also shown to take up exogenous Neu5Gc from the culture medium and incorporate it into cell-surface glycoconjugates, demonstrating that intrinsic biochemical pathways are compatible with Neu5Gc and recognize it biochemically as “self” (26, 27). In striking contrast, the human immune system regards Neu5Gc-containing glycan structures as “foreign,” resulting in a polyclonal humoral response, with circulating and varying titers of anti-Neu5Gc antibodies among all humans (29, 30). The incorporation of dietary Neu5Gc in the face of an ongoing immune response against this non-human epitope makes Neu5Gc the first known example of a “xeno-autoantigen” (31, 32). Interestingly, the major sites of Neu5Gc accumulation in humans (endothelia of blood vessels and epithelia lining the hollow organs) are also the locations where predominantly human-specific diseases involving chronic inflammation seem to occur (31). Notably, such chronic inflammation-mediated human health issues (e.g. atherosclerosis of medium and large vessels or certain epithelial carcinomas) are also associated with the consumption of Neu5Gc-rich foods such as red meats (33–36). Thus, “xenosialitis” has been proposed to be a novel human-specific mechanism, which could exacerbate vascular pathologies such as arteriosclerosis (37), and was found to stimulate tumor growth in a human-like mouse model (38). Investigating the intracellular fate of Neu5Gc may help explain the underlying mechanisms of xenosialitis in humans.

As the CMAH reaction (CMP-Neu5Ac → CMP-Neu5Gc) is irreversible, all mammalian cells must have pathways to adjust cellular Neu5Gc levels to their needs to avoid continued accumulation. Such a metabolic pathway for the turnover of Neu5Gc has not been reported in any system. However, several enzymes involved in sialic acid biosynthesis were previously shown to accommodate both the *N*-acetyl substituent as well as the *N*-glycolyl moiety. Examples include the CMP-sialic acid synthetase from various animals, including humans (39) and mammalian sialyltransferases (40). Moreover, mammalian *N*-acetylneuraminic pyruvate-lyase was found to release pyruvate from Neu5Ac and Neu5Gc to give ManNAc and ManNGc, respectively (41, 42). In this study, we hypothesized that additional enzymes involved in further breakdown of ManNAc and ManNGc may also tolerate the *N*-glycolyl group. Based on the well known metabolism of *N*-acetylhexosamines in mammalian cells, we thus propose a conceivable pathway for the degradation of excess Neu5Gc. We show that the predicted reactions occur in murine tissue cytosolic extracts, demonstrating that mammalian *N*-acetylhexosamine pathways can accommodate the *N*-glycolyl group to some extent allowing degradation of excess Neu5Gc into the two ubiquitous metabolites glycolate and glucosamine 6-phosphate. Further analysis of recombinant human enzymes and studies on the fate of radiolabeled pathway intermediates in cultured human cells indicate that this path-

way likely also persists in humans. The identification of the first Neu5Gc-degrading metabolic pathway in mammals has fundamental implications for sialic acid biochemistry and biology, and it may also have significant impact on the development of strategies to manage Neu5Gc accumulation in humans and its potentially deleterious consequence xenosialitis.

EXPERIMENTAL PROCEDURES

Materials

[1,2-¹⁴C]Glycolic acid was received from ICN Biomedicals, Inc. All chemicals were purchased at HPLC grade from Fisher or Sigma unless otherwise stated.

Generation of Expression Plasmids

The sequence of all primers used in this study can be found in supplemental Fig. S5. Human *NAGK* gene (accession number BC0010029), cloned EcoRI/XhoI in pOTB7 vector was purchased from Thermo Scientific (clone ID 3347484). The gene was amplified by PCR using the primer pair AKB20/AKB21 and the above plasmid as template. The PCR product was cloned via EcoRI/XhoI sites into a modified pGEX-2T expression vector (GE Healthcare, harboring the additional sequence 5'-CCGGTCTGACTCGAGCGGCCGC-3' inserted 3' of EcoRI), resulting in the plasmid pGEX-h*NAGK* to express NagK with an N-terminal GST fusion tag. Human *AMDHD2* gene (accession number BC018734), cloned EcoRI/XhoI in pOTB7 vector was purchased from Thermo Scientific (clone ID 4869721). The gene was amplified by PCR using the primer pair AKB3/AKB9 and the above plasmid as template. The pET22b expression vector (Novagen) was modified by adapter ligation via XbaI/BamHI of primers AKB11/AKB12 to remove the pelB leader sequence. The PCR product was subcloned via NdeI/XhoI sites into the modified pET22b expression vector described above resulting in plasmid pET22b-h*AMDHD2*-His to express *Amdhd2* with a C-terminal hexahistidine tag. The identity of all plasmids was confirmed by sequencing.

Expression and Purification of Recombinant Human GlcNAc Kinase

Plasmid pGEX-h*NAGK* was transformed into BL21(DE3) bacteria, and the protocol for expression and purification was modified from Yamada-Okabe *et al.* and Weihofen *et al.* (43, 44). Freshly transformed bacteria were cultivated at 37 °C in 500 ml of LB medium containing 200 μg/ml carbenicillin. At $A_{600\text{ nm}} = 0.6$, expression was induced by adding 0.3 mM isopropyl β-D-1-thiogalactopyranoside. Thereafter, bacteria were grown at 37 °C for 4 h, pelleted at 6000 × *g* for 10 min at 4 °C, and washed with 20 ml of PBS, and the pellet was kept on ice. Bacteria were resuspended in 20 ml of PBS, lysed by sonication (in ice-water, five times for 30 s pulsed with 0.5 s ON and 0.5 s OFF and 2 min breaks in-between; level 4 on a 550 sonic dismembrator, Fisher), and the membrane fraction was removed at 4 °C/27,000 × *g*/1 h. The supernatant containing soluble expressed GST-NagK was loaded onto a 2-ml glutathione-Sepharose 4B column (GE Healthcare) pre-equilibrated with 10 ml of PBS. After loading, the column was washed successively with 5 ml of PBS and 10 ml of buffer A (20 mM Tris-HCl, pH 7.5, 50

mM NaCl, 1 mM dithiothreitol (DTT)). Bound proteins were eluted with $3 \times 600 \mu\text{l}$ of 10 mM glutathione in buffer A. Eluted fractions were pooled and dialyzed against buffer A using Spectra/Por Dialysis Membrane 6 (MWCO 10,000; Spectrum Laboratories). The enzyme was stored at -80°C and remained active for at least 1 year.

Expression and Purification of Recombinant Human GlcNAc-6-P Deacetylase

Plasmid pET22b-hAMDHD2-His was transformed into BL21(DE3) bacteria. Freshly transformed bacteria were cultivated at 37°C in 500 ml of LB medium containing $200 \mu\text{g/ml}$ carbenicillin. At $A_{600\text{nm}} = 0.6$, expression was induced by adding 1 mM isopropyl β -D-1-thiogalactopyranoside, and the medium was supplemented with 1 mM ZnCl_2 as described previously for the *Escherichia coli* analog NagA (45). Thereafter, bacteria were grown at 15°C for 16 h, pelleted at $6000 \times g$ for 10 min at 4°C , and washed with 20 ml of PBS, and the pellet was kept on ice. Bacteria were resuspended in loading buffer (50 mM Tris-HCl pH 7.5, 100 mM NaCl, 20 mM imidazole, 1 mM DTT) supplemented with $100 \mu\text{g/ml}$ phenylmethanesulfonyl fluoride (PMSF) and lysed by sonication (on ice-water, five times for 30 s pulsed with 0.5 s ON and 0.5 s OFF and 2 min breaks in between; level 4 on a 550 sonic dismembrator, Fisher), and the membrane fraction was removed at $4^\circ\text{C}/27,000 \times g/1 \text{ h}$. The supernatant containing soluble expressed Amdhd2-His was loaded onto a 1-ml HisTrapHP column (GE Healthcare) pre-equilibrated with loading buffer. Bound proteins were eluted with a 20 ml linear imidazole gradient (20–500 mM imidazole in loading buffer; flow rate 1 ml/min) by FPLC. Enzyme-containing fractions were pooled and dialyzed against storage buffer (50 mM Tris-HCl pH 7.5, 100 mM NaCl, 1 mM DTT) using Spectra/Por dialysis membrane 6 (MWCO 10,000; Spectrum Laboratories). The enzyme was either stored flash-frozen at -80°C or in 50% glycerol at -20°C and remained active for at least 1 year.

SDS-PAGE, Coomassie Staining, and Immunoblotting

SDS-PAGE was performed under reducing conditions using 2.5% (v/v) β -mercaptoethanol. Coomassie staining and Western blot analysis with anti-penta-His antibody (Qiagen) were performed as described previously (46).

HPLC Analysis Using HPAEC-PAD Followed by Scintillation Counting

Monosaccharides were separated by HPLC (Dionex DX-600 BioLC system equipped with an ED50 Electrochemical Detector, Dionex) using a CarboPac PA-1 column (Dionex) under alkaline conditions. Samples ($100 \mu\text{l}$) were injected, and the developed gradient described in supplemental Fig. S2 was applied at a flow rate of 1 ml/min. Following HPAEC-PAD detection, 0.5-ml fractions were collected directly into scintillation vials whenever radiolabeled material was analyzed. To each vial, 5 ml of scintillation mixture was added (Scinti Verse BD, Fisher) prior to measuring on a scintillation counter. Because of the lack of qualified hydroxyl groups, glycolic acid cannot be detected by HPAEC-PAD. However, co-elution of commercial [^{14}C]glycolic acid and synthesized [^3H]glycolic

acid is observed at 13.5 ml using the gradient described in supplemental Fig. S2.

Activity Assay for Human GlcNAc Kinase

Assay conditions were modified from Yamada-Okabe and co-workers (43). The assay contained 50 mM Tris-HCl pH 7.5, 10 mM MgCl_2 , 5 mM DTT, 5 mM ATP, 1 mM of either GlcNAc or GlcNGc, and 0.22 nmol of purified enzyme in a total volume of $50 \mu\text{l}$. As a background control, the reaction was set up without the substrates GlcNAc or GlcNGc. After 1 h of incubation at 37°C , the reaction mixtures were spun through Amicon Ultra-0.5 ml 10K Ultracel filter units (Millipore) to remove the enzyme prior to analysis by HPLC following HPAEC-PAD.

Activity Assays for Human GlcNAc-6-P Deacetylase

1) Enzyme activity assays were carried out in $30 \mu\text{l}$ volumes containing 25 mM Tris-HCl pH 7.5, 1 mM DTT, either 5 mM GlcNAc-6-P or 5 mM GlcNGc-6-P, and 0.3 nmol of purified recombinant human deacetylase. Before and after incubation at 37°C for 1 h, $10 \mu\text{l}$ of the reaction mixtures were spotted on 3MM CHR Whatman chromatography paper. Subsequently, separation was achieved by descending paper chromatography using running buffer (3 volumes ethanol and 7 volumes of 1 M ammonium acetate, pH 3.9) as described previously (47). The separated sugars on the chromatogram were detected by silver staining using a modified version of the protocol from Trevelyan *et al.* (48). In brief, the dried paper chromatogram was quickly and evenly dipped through a trough containing solution A (0.1 ml of saturated aqueous silver nitrate solution in 20 ml of acetone). After air-drying, the paper was dipped through solution B (20 mg of NaOH in just enough water to dissolve it, and methanol was added to a final volume of 1 liter). Once color has developed sufficiently, the staining was fixed by passing through solution C (31.8 mg of sodium thiosulfate first dissolved in 475 ml of water followed by addition of 475 ml of methanol). 2) An additional activity assay was set up in a $210\text{-}\mu\text{l}$ final volume containing 25 mM Tris-HCl pH 7.5, 1 mM DTT, either 2 mM GlcNAc-6-P or 2 mM GlcNGc-6-P, and 0.9 nmol of purified recombinant human deacylase at 37°C . Control reactions were set up by adding heat-inactivated enzyme (5 min/ 95°C) to the reaction mixtures. Aliquots ($30 \mu\text{l}$) were removed from the reaction mixtures after 30 s, 1, 5, 15, and 30 min, and 1 h and transferred into tubes harboring $70 \mu\text{l}$ of pre-cooled ethanol to quench the reaction. Precipitation was allowed to occur overnight at -20°C . Thereafter, samples were spun at $20,000 \times g/15 \text{ min}/4^\circ\text{C}$, and the supernatants were transferred into clean tubes and dried. For subsequent HPLC analysis, samples were resuspended in $110 \mu\text{l}$ of water, filtered, and analyzed as described above.

Mice

WT C57BL/6 mice were purchased from Harlan Laboratories. *Cmah*^{-/-} mice have been described previously (18). Mice were fed standard chow (PicoLab Rodent Diet 20; LabDiet) and water *ad libitum* and maintained on a 12-h light/dark cycle. All animal work was performed in accordance with The Association for Assessment and Accreditation of Laboratory Animal Care under protocol S01227 approved by The Institutional

Metabolic Fate of N-Glycolylneuraminic Acid

Animal Care and Use Committee of the University of California San Diego.

Preparation of *Cmah*^{-/-} Mouse Embryonic Fibroblasts

To generate *Cmah*^{-/-} fibroblasts, 14- to 17-day-old embryos of a *Cmah*^{-/-} mouse (18) were dissected by removing the amniotic sac and the placenta from the embryo. Blood was removed by repetitive washing in PBS, and thereafter, the carcasses were minced with scissors. Per embryo, 3–5 ml of 0.05% trypsin/EDTA solution (Invitrogen) were added and incubated at 4 °C overnight to allow diffusion of the trypsin into the tissue. The next day, without disturbing the pellet of tissue, most of the trypsin solution was removed, and the tissue pellet was incubated at 37 °C for 60 min. Thereafter, the pellet was carefully resuspended in 50 ml of fresh Dulbecco's modified Eagle's medium (DMEM) supplemented with 10% FCS. The sample was spun at 1000 rpm for 1 min to let the remaining tissue clumps accumulate at the bottom of the tube. The supernatant was transferred to a clean tube and spun for 5 min at 1000 rpm to pellet cells. The supernatant was aspirated, and the cell pellet was resuspended in fresh media. Cells derived from 3 to 4 embryos were plated in a T-175 flask, and the media were changed the next day. The cells were passaged upon reaching confluency.

Production of the retrovirus was conducted based on previously described methods (49). The packaging cell line PA317 LXSNI6E6E7 developed by transfection of the retroviral vector pLXSNI6E6E7, which contains the human papilloma virus as well as a gene controlling resistance to neomycin, was purchased from ATCC. These cells were grown in DMEM with 4 mM L-glutamine adjusted to contain 1.5 g/liter sodium bicarbonate, 4.5 g/liter glucose, and 10% fetal bovine serum. The cells were grown to 70–80% confluency, and the supernatant was collected after 16 h. The supernatant was filter-sterilized through a 0.22- μ m filter and stored at -80 °C. The supernatant was then used for transduction to immortalize *Cmah*^{-/-} fibroblasts based on previous protocols (50). Briefly, *Cmah*^{-/-} fibroblast cells were seeded at 3×10^5 cells per T-75 flask and allowed to adhere overnight. Transduction of the cells was accomplished by using 1 ml of the sterile-filtered supernatant containing the human papilloma virus in the presence of 8 μ g/ml Polybrene in a total volume of 10 ml for 8 h at 37 °C in a 5% CO₂-humidified incubator. The media containing the virus were removed and replaced with fresh medium (DMEM high glucose supplemented with 10% FCS, 25 units/ml penicillin, 25 units/ml streptomycin) and grown for 3 days. Transduced cells were selected by adding 100 μ g/ml G418 for 14 days.

Tissue Culture

Human acute monocytic leukemia cell line THP-I (51) and murine *Cmah*^{-/-} fibroblasts were cultivated in DMEM (high glucose, Invitrogen); human M-21 cells (52) were grown in α -minimal essential medium, and human B lymphoma cell line BJA-B (Burkitt's lymphoma-like (53), subclones K88 and K20 (54)) were kept in RPMI 1640 medium. All media were supplemented with 5% Neu5Gc-free human serum (heat-inactivated and sterile-filtered, Valley Biomedical Inc.) and 2 mM gluta-

mine. Cells were cultivated in a humidified 5% CO₂ atmosphere at 37 °C.

Feeding of Animal Cells

For feedings of suspension cells (THP-I or BJA-B), 1×10^6 cells were set up in a well of a 6-well dish in a final volume of 2 ml of feeding media as described below. Adherent cells (*Cmah*^{-/-} fibroblasts, M-21 cells) were split into P-100 dishes in a manner to reach confluency after 4 days again and allowed to attach overnight. The next day, the media were removed; cells were washed with PBS, and 5 ml of feeding media were added as described below. The feeding media were supplemented with compounds as indicated using the following pH neutral and sterile-filtered stock solutions either prepared in PBS, pH 7.4 (100 mM Neu5Gc, 1 M glycolic acid, 1 M GABA, 1 M ManNGc, and 1 M GlcNGc), or dissolved in DMSO (100 mM GlcNGc, 100 mM per-*O*-acetyl-GlcNGc, 100 mM ManNGc, and 100 mM per-*O*-acetyl-ManNGc). Regarding cell feedings with ManNGc and GlcNGc, the DMSO stock was used when aiming for a final concentration of 100 μ M in the media. The PBS stock was used to set up feeding media with a 10 mM final concentration of the compounds. Cells were kept in the feeding media for 3 days. Adherent cells were detached with 20 mM EDTA in PBS first, and all cells were washed three times with PBS. Cells were analyzed by flow cytometry as described below.

For the pulse-chase experiment (Fig. 2A), 1×10^7 THP-I cells were incubated in 10 ml of fresh media supplemented with 5 mM Neu5Gc for 3 days. Thereafter, the cell pellet was washed three times with PBS, resuspended in 20 ml of fresh media, and split equally into 10 wells of 6-well dishes (2 ml/well). All cells of a well were harvested at days 0 and 1–6. At day 6 of the chase, all remaining wells were diluted 1:3 in fresh media individually and transferred into T-75 flasks. At day 14, all cells of one T-75 flask were harvested, and the remaining two T-75 flasks were further diluted 1:3. At day 21, all cells of one T-75 flask were harvested, and the last T-75 flask was again diluted 1:3, and all cells were harvested on day 28. Cell pellets were washed three times with PBS and frozen at -80 °C. After all time points were collected, Neu5Gc content of total cell lysates was determined by DMB-HPLC as described below.

Radiolabeled Cell Feedings

THP-I cells (1×10^6 cells, 2 ml of culture medium in a well of a 6-well dish) were incubated for 3 days in the presence of 370 kBq [³H]ManNGc, 370 kBq [³H]GlcNGc, or 74 kBq [³H]glycolic acid. *Cmah*^{-/-} fibroblasts were cultured in a P-100 dish, and 3 days prior to reaching confluency, the media were removed; cells were washed, and 5 ml of fresh medium supplemented with 110 kBq [³H]glycolic acid was added. After 3 days, cells were harvested using 20 mM EDTA in PBS. All radiolabeled cells were washed three times with PBS, and pellets were stored at -20 °C. For analysis, cell pellets were resuspended in 30 μ l of 10 mM Tris-HCl, pH 7.5, and lysed by repetitive freeze-thaw. Proteins and membrane debris were precipitated by addition of 70 μ l of ethanol (70% final) at -20 °C overnight. Mixtures were spun for 20 min at 20,000 $\times g$ at 4 °C; the supernatants were transferred into fresh tubes, and samples

were dried down. For HPLC analysis, samples were resuspended in a final volume of 110 μl of water (supplemented with internal standards whenever mentioned), filtered, and analyzed as described above.

Flow Cytometry

For staining, cells were resuspended in blocking solution (PBS pH 7.4, supplemented with 0.5% gelatin from cold water fish skin (Sigma) and 2 mM EDTA) containing either a 1:10,000 dilution of polyclonal monospecific chicken anti-Neu5Gc antibody (anti-Neu5Gc IgY (25)) or control chicken IgY (Jackson ImmunoResearch). Cells were incubated for 1 h on ice. Thereafter, cells were pelleted and resuspended in blocking solution containing a 1:4000 dilution of Cy5-conjugated donkey anti-chicken IgY antibody (Jackson ImmunoResearch). Cells were incubated for 1 h on ice, pelleted, and resuspended in blocking solution for subsequent analysis. Data were collected on a FACSCalibur flow cytometer (BD Biosciences) and analyzed using the FlowJo software (Tree Star).

DMB-HPLC

DMB-HPLC was performed as described in the companion paper (28). As starting material, ~5% of cells from a confluent P-100 dish or 100 μl of a dense suspension cell culture were used in the protocol. Cell lysates were prepared by repetitive freeze-thaw followed by sonication. For the pulse-chase experiment with THP-I cells (Fig. 2A), 90% (days 0–6), 45% (days 14 and 21), and 22.5% (day 28) of total cell lysate, respectively, were used for DMB-HPLC analysis. Resulting sialic acid amounts were corrected for the dilution factor thereafter.

Preparation of Cytosolic Extracts from Mouse Liver

A whole mouse liver (C57/BL6, ~0.8 g) was harvested and minced with scissors in pre-cooled 2.4 ml of PBS pH 7.4, on ice. The tissue was homogenized using a Polytron (Brinkmann Instruments) for 30 s at medium speed on ice and subsequently spun at $100,000 \times g$ for 1.5 h at 4 °C. The supernatant was recovered and represents the cytosolic extract. Beforehand, 50,000 cpm (1.31 kBq) of radiolabeled monosaccharides were dried down in tubes and now resuspended in 50 μl of the fresh cytosolic liver extract. Remaining tissue extract was kept on ice. Where mentioned, 5 mM ATP (along with 10 mM MgCl_2) was added to the sample, and all reaction mixtures were incubated at 37 °C for 6 h. Thereafter, reactions were either quenched with ethanol immediately or supplemented with 5 mM ATP (along with 10 mM MgCl_2) and extra 50 μl of cytosolic extracts for an additional 6 h incubation at 37 °C if mentioned in the text. To quench reactions, pre-cooled ethanol was added to a final concentration of 70%, and precipitation was allowed to occur at –20 °C overnight. Thereafter, samples were spun at $20,000 \times g$ for 15 min at 4 °C. The supernatant was transferred into clean tubes and dried down. For subsequent HPLC analysis, samples were resuspended in a final volume of 110 μl of water (supplemented with internal standards where it applied), filtered, and analyzed as described above.

Chemical Methods

General

“Brine” refers to a saturated aqueous solution of sodium chloride. Proton nuclear magnetic resonance spectra (d_{H}) were recorded on a Jeol ECA 500 (500 MHz). 500 MHz spectra were assigned using COSY. All chemical shifts are quoted on the δ -scale in ppm, using residual solvent as the internal standard. Low resolution mass spectra, obtained at the University of California San Diego, Chemistry and Biochemistry Molecular MS Facility, were recorded on a Micromass Platform 1 spectrometer using electron spray (ES) ionization with methanol as carrier solvent. Flash column chromatography was performed using Sorbsil C60 40/60 silica gel. Thin layer chromatography (tlc) was performed using Merck Kieselgel 60F254 pre-coated aluminum backed plates. Plates were visualized using 5% sulfuric acid in methanol.

Generalized Method to Prepare 2-Deoxy-2-[(hydroxyacetyl)amino]-D-pyranose (ManNGc and GlcNGc)

2-Amino-2-deoxy-D-glycopyranoside hydrochloride salt (1.4 g, 6.5 mmol) was dissolved in water (60 ml) with sodium bicarbonate (10.8 g, 130 mmol) and cooled in an ice bath. Acetoxyacetyl chloride (4.2 ml, 39 mmol) was added slowly to the reaction mixture. After 30 min tlc (EtOAc/MeOH, 7:3) showed complete consumption of the starting material (R_f 0.0) and the formation of the product (approximate R_f 0.3). The reaction mixture was neutralized with mixed bed resin. Finally, the product was purified through silica column and concentrated under vacuum to yield a white gum (1.4 g, 5.9 mmol, 91%).

2-Deoxy-2-[(hydroxyacetyl)amino]-D-mannopyranose (ManNGc)—Spectral data are in good agreement with a published report (55).

2-Deoxy-2-[(hydroxyacetyl)amino]-D-glucopyranose (GlcNGc) (56)—For ^1H NMR (D_2O , 500 MHz) (assigned for the major anomer), δ = 3.31 (t, J = 3.6 Hz, 1H), 3.34 (t, J = 9.6 Hz, 1H), 3.64 (t, J = 9.7 Hz, 1H), 3.67 (t, J = 3.4 Hz, 1H), 3.72 (m, 1H), 3.78 (dd, $J_{1,2}$ = 3.7 Hz, $J_{2,3}$ = 10.9 Hz, 1H), 3.96 (s, 2H), 5.04 (d, $J_{1,2}$ = 3.7 Hz, 1H). m/z (ESI $^+$) was 260 (M + Na $^+$, 100%). The HRMS m/z (ES $^+$) calculated for $\text{C}_8\text{H}_{15}\text{NO}_7\text{Na}$ (M + Na $^+$) was 260.0741 and found was 260.0743.

Generalized Method to Make 1,3,4,6-Tetra-O-acetyl-2-deoxy-2-[(acetoxyacetyl)amino]-D-glycopyranose (Per-O-acetyl-ManNGc and Per-O-acetyl-GlcNGc)

2-Deoxy-2-[(hydroxyacetyl)amino]-D-glycopyranose (200 mg, 0.80 mmol) was slurried in acetic anhydride (5 ml) and pyridine (5 ml). After 24 h, tlc (EtOAc/petrol, 1:9) showed complete consumption of the starting material (R_f = 0.0). The clear/colorless solution was dried under reduced pressure to yield a sticky straw-colored gum. The residue was dissolved in chloroform and washed with sodium bicarbonate, water, and finally brine. The solution was then dried with sodium sulfite, filtered, and dried under vacuum to yield a white gum. The crude product was purified through silica column and dried under vacuum to yield a clear colorless gum. (320 mg, 0.71 mmol, 90%).

Metabolic Fate of N-Glycolylneuraminic Acid

1,3,4,6-Tetra-O-acetyl-2-deoxy-2-[(acetoxy-acetyl)amino]-D-mannopyranose (Per-O-acetyl-ManNGc) (57)—¹H NMR (CD₃Cl, 500 MHz) (assigned for the major anomer) was as follows: δ = 1.99 (s, 3H, CH₃), 2.05 (s, 3H, CH₃), 2.09 (s, 3H, CH₃), 2.18 (s, 3H, CH₃), 2.20 (s, 3H, CH₃), 4.03–4.07 (m, 1H), 4.24 (dd, *J* = 12.8, *J* = 4.8, 1H), 4.60 (s, 2H), 4.76 (ddd, *J* = 9.1, *J* = 3.7, *J* = 1.7, 1H), 5.16 (t, *J* = 10.1, 1H), 5.31 (dd, *J* = 4.6, *J* = 10.4, 1H), 6.03 (d, *J* = 2.0, 1H), 6.41 (d, *J* = 9.1, 1H). *m/z* (ESI⁺) was 470 (M + Na⁺, 100%), 465 (M + NHMACROS BELOW ARE FOR THE VISUAL₄⁺, 10%). The HRMS *m/z* (ES⁺) calculated for C₁₈H₂₅NO₁₂Na (M + Na⁺) was 470.1269 and found was 470.1270.

1,3,4,6-Tetra-O-acetyl-2-deoxy-2-[(acetoxy-acetyl)amino]-D-glucopyranose (per-O-acetyl-GlcNGc) (56)—¹H NMR (CD₃Cl, 500 MHz) (assigned for the major anomer) is as follows: δ = 2.04 (s, 3H, CH₃), 2.04 (s, 3H, CH₃), 2.08 (s, 3H, CH₃), 2.16 (s, 3H, CH₃), 2.19 (s, 3H, CH₃), 3.97–4.01 (m, 1H), 4.04 (dd, *J* = 2.3, *J* = 12.6, 1H), 4.23 (dd, *J* = 12.6, *J* = 4.0, 1H), 4.43 (m, 2H), 4.57 (s, 2H), 5.19–5.28 (m, 1H), and 6.22 (d, *J* = 3.7, 1H, H-1). *m/z* (ESI⁺) was 470 (M + Na⁺, 100%), 465 (M + NH₄⁺, 10%). The HRMS *m/z* (ES⁺) calculated for C₁₈H₂₅NO₁₂Na (M + Na⁺) was 470.1269 and found was 470.1271.

Method to Prepare 2-Deoxy-2-[(hydroxyacetyl)amino]-6-phosphate-D-glucopyranose (GlcNGc-6-P) (58)

To glucosamine 6-phosphate in phosphate-buffered saline (pH 7.4, 50 mM, 1 ml) was added (final concentration) glycolic acid (250 mM), *N*-hydroxysulfosuccinimide (sulfo-NHS, 5 mM), and ethyl-3-(3-dimethylaminopropyl)-carbodiimide (EDC, 100 mM). The reaction was incubated at RT for 30 min, after which water (10 ml) was added. The product was purified by ion-exchange column (Dowex 50 H⁺ form, 2 ml; Bio-Rad). The column was washed with water (5 ml). The flow-through and the wash were collected and passed through a second ion-exchange column (AG 50W-X8, 2 ml; Bio-Rad). The column was washed with water (10 ml) and formic acid (1 M, 10 ml). The product was eluted from the column using formic acid (5 M, 10 ml). The eluate was dried under reduced pressure to yield a clear colorless gum. ¹H NMR (D₂O, 500 MHz) (assigned for the major anomer) is as follows: δ = 3.47 (t, *J* 9.5 Hz, 1H), 3.52 (dd, *J* 4.0 Hz, *J* 9.8 Hz, 1H), 3.64 (t, *J* 9.7 Hz, 1H), 3.69 (t, *J* 9.4 Hz, 1H), 3.85 (dd, *J* 4.0 Hz, *J* 10.6 Hz, 1H), 3.93 (dd, *J* 4.1 Hz, 10.9 Hz, 1H), 4.00 (s, 2H), 5.08 (d, *J*_{1,2} 3.6 Hz, 1H). *m/z* (ESI⁻) 316 (M - H⁺, 100%), 338 (M + Na-2H⁺, 30%). The HRMS *m/z* (ES⁺) calculated for C₈H₁₆NO₁₀PNa (M + Na⁺) was 340.0404 and found was 340.0406.

Preparation of [³H]Glycolic Acid

[³H]Glycolic acid was synthesized from [³H]NaBH₄ and glyoxylate. Commercial solid [³H]NaBH₄ (PerkinElmer Life Sciences, 37 GBq, 2.442 GBq/μmol) was resuspended in 250 μl of 1 mM NaOH, whereupon 100 μl (14.8 GBq) were used in the following. A 500 mM glyoxylate stock solution was prepared (pH 8.0), and 69 μl were added to the [³H]NaBH₄. The reaction mixture was incubated at room temperature for 1.5 h and thereafter quenched by adding 3.8 μl of acetone. After incubation for another hour at room temperature, the sample was diluted to 2.5 ml with water and then purified by polyethyleneimine (PEI)

chromatography to remove excess glyoxylate. The diluted sample was loaded onto a 3 ml column of PEI-cellulose, pre-equilibrated in water. The column was washed with 30 × 6 ml of water, washed with 3 × 6 ml of 40 mM NaCl, and eluted with 3 × 6 ml of 100 mM NaCl. The recovery was monitored by scintillation counting of diluted aliquots of each of the wash and eluate fractions. The pooled eluate of 18 ml was stored frozen. The final yield was ~85% (12.6 GBq), and the identity of synthesized [³H]glycolic acid was confirmed by HPLC, observing co-elution with commercial [¹⁴C]glycolic acid.

Preparation of [glycolyl-³H]ManNGc and [glycolyl-³H]GlcNGc

To synthesize [glycolyl-³H]ManNGc, 4 GBq of prepared [³H]glycolic acid were incubated with 50 mM mannosamine in the presence of 50 mM EDC and 2.5 mM sulfo-NHS in 50 mM MOPS buffer pH 7.5, in a final volume of 8 ml. Synthesis of [glycolyl-³H]GlcNGc was achieved in the same manner using 0.63 GBq of prepared [³H]glycolic acid and 50 mM glucosamine. The reaction mixtures were incubated overnight at room temperature with gentle mixing, subsequently diluted to 20 ml with water, and applied to 5 ml Dowex-50 columns (AG 50W-X2, Bio-Rad) pre-equilibrated with water. The columns were washed with 5 CV water; the washes were pooled with the run-through, and the pools were applied onto 5 ml of AG3X4A (OH⁻ form, Bio-Rad) columns pre-equilibrated with water. The columns were washed with 5 CV water, and the washes were pooled with the run-through. The pools containing the synthesized [glycolyl-³H]ManNGc and [glycolyl-³H]GlcNGc, respectively, were adjusted to 50% ethanol and stored at -20 °C. The preparations were diluted to prevent autoradiolysis. The recovery was monitored by scintillation counting, and the final yields of [glycolyl-³H]ManNGc and [glycolyl-³H]GlcNGc were 0.84 GBq (21.0%) and 0.27 GBq (43.2%), respectively. The identity of synthesized [glycolyl-³H]ManNGc and [glycolyl-³H]GlcNGc was confirmed by HPLC, demonstrating co-elution with their nonlabeled chemically well characterized counterparts.

Preparation of [¹⁴C]GlcNGc

To synthesize [¹⁴C]GlcNGc, 1.85 MBq of D-[U-¹⁴C]glucosamine hydrochloride (Amersham Biosciences, in 3% ethanol) were dried down on a shaker evaporator. The dry material was then incubated with 50 mM glycolic acid in the presence of 50 mM EDC and 2.5 mM sulfo-NHS in 50 mM MOPS, pH 7.5, in a final volume of 100 μl. The sample was processed as described above for preparation of [glycolyl-³H]GlcNGc, but a 1-ml Dowex-50 column was used here. The final yield of [¹⁴C]-GlcNGc was 0.98 MBq (53.0%), and the identity was confirmed by HPLC, demonstrating co-elution with [glycolyl-³H]GlcNGc.

Preparation of [glycolyl-³H]GlcNGc-6-P

The [glycolyl-³H]GlcNGc-6-P was prepared from [³H]glycolic acid and GlcNH₂-6-P. In a 200-μl final volume, 3.7 MBq of [³H]glycolic acid were incubated in the presence of 10 mM GlcNH₂-6-P, 100 mM EDC, and 5 mM sulfo-NHS in PBS, pH 7.5. The reaction mixture was incubated for 15 min at room temperature and thereafter diluted to 1 ml with water. Subse-

quently, the sample was applied onto a 1 ml Dowex-50 (AG-50W-X2) column pre-equilibrated with water. The column was washed with 5 CV of water, and the run-through was pooled with the water washes. This pool was applied onto a 1 ml Dowex-1 column (AG-1-X8), pre-equilibrated with water. The column was washed with 5 CV water followed by 5 CV of 1 M formic acid. The [*glycolyl*-³H]GlcNGc-6-P was subsequently eluted with 5 CV of 5 M formic acid. The formic acid was driven off by using a shaker evaporator. The final yield of synthesized [*glycolyl*-³H]GlcNGc-6-P was 0.392 MBq (10.6%), and the identity of the compound was confirmed by HPLC, revealing co-elution with chemically well characterized nonlabeled GlcNGc-6-P.

Preparation of [*glycolyl*-³H]Neu5Gc

Previously described protocols for synthesis of radiolabeled Neu5Gc (59) have been modified to achieve a compound exclusively labeled in the *N*-glycolyl group. The [*glycolyl*-³H]Neu5Gc was prepared from [*glycolyl*-³H]ManNGc by enzymatic conversion using the *N*-acetylneuraminase pyruvate-lyase (EC 4.1.3.3) from *Pasteurella multocida*. A His₆-tagged version of the enzyme was recombinantly expressed and purified as described previously (60). In a total volume of 100 μl, 456 MBq [*glycolyl*-³H]ManNGc were incubated with 33.67 μg of purified *N*-acetylneuraminase pyruvate-lyase in the presence of 100 mM Tris-HCl, pH 7.5 and 200 mM sodium pyruvate. The reaction was incubated at 37 °C for 20 h with mixing and thereafter quenched by diluting to 5 ml with water. The [*glycolyl*-³H]Neu5Gc was purified from nonreacted [*glycolyl*-³H]ManNGc by passing the sample through a 2 ml column of AG-50-X2 (H⁺ form). The flow-through and 5 CV water washes were collected and combined. This effluent was then loaded onto a 2 ml column of AG-1-X8 (formate form) equilibrated in water. The column was washed with 5 CV of water followed by 7 ml of 10 mM formic acid and finally eluted into a separate tube with 10 ml of 1 M formic acid. The eluate was dried down to remove formic acid. The final [*glycolyl*-³H]Neu5Gc preparation was dissolved in water. Recovery was followed by counting an aliquot of each fraction at each step of the purification process. Final yield was found to be 70 MBq (15.4%). The identity of [*glycolyl*-³H]Neu5Gc was confirmed by co-elution with commercial Neu5Gc (Inalco) by HPLC as described above.

RESULTS AND DISCUSSION

Embryonic Fibroblasts from *Cmah*^{-/-} Mice Do Not Synthesize Neu5Gc—CMAH is the only enzyme currently known to synthesize Neu5Gc (6–13). Early studies of other possible alternative pathways suggested the lack of involvement of hydroxy-pyruvate or glycolyl-CoA in the biosynthesis of the *N*-glycolyl group of Neu5Gc (61). Despite this, the presence of Neu5Gc in some human tissues and tumors caused others to again raise the possibility of such alternate pathways for Neu5Gc *de novo* biosynthesis (62, 63). However, tissues from *Cmah*^{-/-} mice with a human-like defect in the gene encoding CMAH were found to be devoid of staining with a polyclonal mono-specific anti-Neu5Gc chicken IgY antibody (anti-Neu5Gc IgY) (18), which is known to detect all types of Neu5Gc-bearing glycans studied so

far (25). This indicates that hydroxylation of CMP-Neu5Ac catalyzed by the CMAH enzyme may be the only pathway for *de novo* biosynthesis of Neu5Gc in mammals. To further investigate this matter on a cellular level and finally rule out the existence of additional pathways for *de novo* biosynthesis of Neu5Gc in mammals, we generated embryonic fibroblasts from *Cmah*^{-/-} mice that were immortalized using a human papilloma virus (49, 50) as described under “Experimental Procedures.” When these cells were cultured in the presence of fetal calf serum (FCS), they did show low levels of Neu5Gc (1.0% of total Sias as analyzed by DMB-HPLC as well as glycosidically bound cell-surface Neu5Gc, as detected by flow cytometry using the anti-Neu5Gc IgY (Fig. 1A)). However, this Neu5Gc likely originates from bovine glycoconjugates present in the FCS (27). The Neu5Gc content of these cells could be rendered even higher when the feeding media were supplemented with 5 mM free Neu5Gc (81.3% of total Sias as analyzed by DMB-HPLC and becoming easily detectable by flow cytometry (Fig. 1A)). In both instances, the Neu5Gc is likely taken up via macropinocytosis and delivered to the cytosol via the lysosomal sialin transporter (27). When the same cells were instead cultured under Neu5Gc-free conditions as described under “Experimental Procedures,” there was a complete absence of detectable Neu5Gc by DMB-HPLC (less than 0.1% Neu5Gc in total sialic acids, which represents the lower limit of detection above background). Taken together, these results clearly indicate that *de novo* biosynthesis of Neu5Gc in mouse cells is dependent on the presence of a functional CMAH enzyme.

Exogenous Glycolate Does Not Contribute to the *N*-Glycolyl Group of Neu5Gc in CMAH-deficient Human or Mouse Cells—Even though humans lack a functional CMAH enzyme, the presence of Neu5Gc has been conclusively shown especially on various human cancer types (24, 26, 38, 64). Although early studies did not favor the idea (61), other authors subsequently again raised the possibility that glycolyl-CoA might contribute to *de novo* biosynthesis of Neu5Gc in various human tumors (24, 62, 63). To re-address this matter, *Cmah*^{-/-} fibroblasts and human THP-I cells were cultured under Neu5Gc-free conditions, and the feeding media were then supplemented with 10 mM free glycolic acid. Analysis of total cell lysates was performed by DMB-HPLC, and no Neu5Gc could be detected. In line with these results, no cell-surface glycosidically bound Neu5Gc was detectable by flow cytometry analyses with anti-Neu5Gc IgY (Fig. 1, B–C). In parallel studies, [³H]glycolic acid was synthesized as described under “Experimental Procedures” and used to supplement the Neu5Gc-free media of *Cmah*^{-/-} fibroblasts and human THP-I cells. Free and bound monosaccharides were prepared from these cells, and unlabeled Neu5Gc was added as an internal standard. Subsequently, samples were analyzed by HPLC followed by HPAEC-PAD and scintillation counting in parallel. The overlays of the resulting elution spectra revealed no significant peak of [*glycolyl*-³H]Neu5Gc in either of the samples (supplemental Fig. S3 and Fig. S4). However, various other unknown radiolabeled peaks were detected, confirming that [³H]glycolic acid was taken up and metabolically utilized by the cells. Furthermore, when the human melanoma cell line M-21 was incubated with glycolic acid under Neu5Gc-free conditions and analyzed by the most sensitive

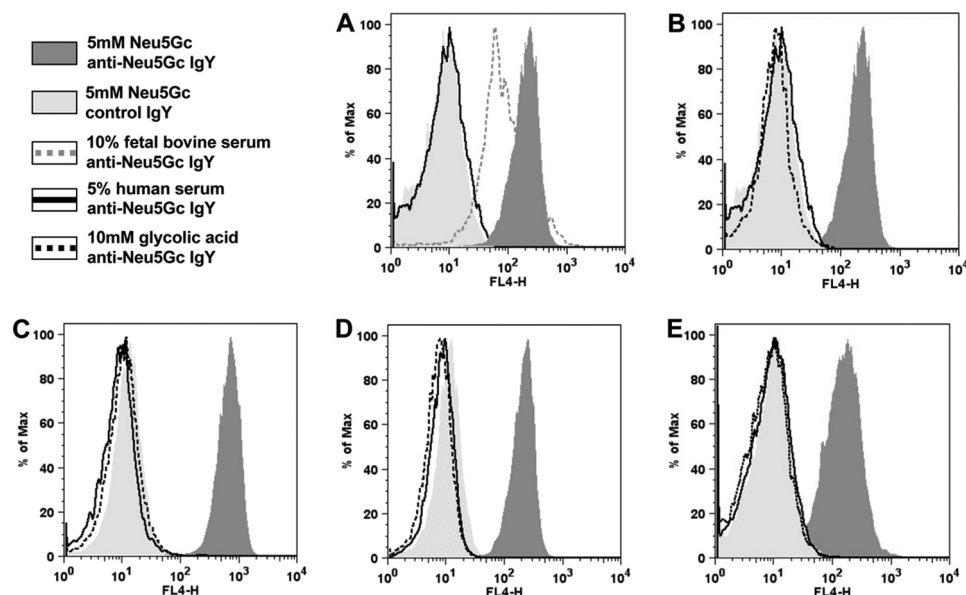


FIGURE 1. CMAH-deficient human and mouse cells do not synthesize Neu5Gc *de novo*. *A*, murine *Cmah*^{-/-} fibroblasts were cultivated under Neu5Gc-free conditions using 5% human serum. Thereafter, the feeding media were supplemented with either 5 mM Neu5Gc (positive control; shaded dark gray) or human serum was substituted by 10% fetal calf serum (FCS; dotted dark gray) to analyze if cells are capable of incorporating exogenous Neu5Gc from the medium supplement FCS. In parallel, cells were kept in 5% human serum without feeding (negative control; black line). After 3 days of feeding, cells were harvested and analyzed by flow cytometry using the polyclonal chicken anti-Neu5Gc antibody (anti-Neu5Gc IgY (25)) for sensitive detection of cell-surface glycosidically bound Neu5Gc. As an additional negative control, cells fed 5 mM Neu5Gc were also stained with control chicken IgY antibody (control IgY; shaded light gray) to verify the absence of Neu5Gc on *Cmah*^{-/-} fibroblasts. *B*, to investigate whether increased glycolic acid levels will result in *de novo* biosynthesis of Neu5Gc in Neu5Gc-deficient *Cmah*^{-/-} fibroblasts, cells were also fed with 10 mM glycolic acid in the media. Cells were treated and detected for Neu5Gc by flow cytometry in parallel to all controls as described above. Also, human THP-1 cells (*C*), M-21 cells (*D*), and human B-cell lymphoma cells BJA-B K20 (*E*) were analyzed for their ability to express cell-surface Neu5Gc after feeding with 10 mM glycolic acid by flow cytometry as described above.

method (flow cytometry), these cells were also found to be devoid of Neu5Gc (Fig. 1*D*). Finally, we studied the human B-cell lymphoma cell line BJAB-K20, which lacks UDP-GlcNAc 2'-epimerase activity (54) and consequently does not synthesize its own sialic acids. This cell line should better reveal any minor alternative *de novo* biosynthetic pathway to yield Neu5Gc, because of the lack of competition by the major CMP-Neu5Ac-based pathway in these cells. However, in line with our previous experiments, no detectable amount of cell-surface Neu5Gc was found by flow cytometry using the anti-Neu5Gc IgY, with or without addition of glycolic acid (Fig. 1*E*). Taken together, these data indicate that glycolic acid does not serve as a precursor for Neu5Gc in CMAH-deficient human and mouse cells and that CMAH is likely the only endogenous source of Neu5Gc production in mammalian cells. However, increased levels of γ -aminobutyric acid (GABA) have been found in various tumors (65–68), an additional precursor of glycolyl-CoA. This led to the hypothesis that Neu5Gc might only be re-expressed under certain metabolic conditions found in tumors. To model this situation, the cell lines THP-1, *Cmah*^{-/-} fibroblasts, M-21, and BJA-B K20 described above were grown under Neu5Gc-free conditions prior to exposing them to 10 mM free GABA and analyzed by flow cytometry with anti-Neu5Gc IgY (supplemental Fig. S1). Again, none of the cell lines was capable of synthesizing detectable amounts of Neu5Gc. Thus, addition of free GABA in high concentrations does not result in re-expression of Neu5Gc in CMAH-deficient mouse cells or in multiple malignant human cell lines, making it highly unlikely that this pathway exists in human tumors.

Elimination of Neu5Gc in Neu5Gc-loaded Cells Over Time— Given the irreversible nature of the CMAH reaction (CMP-

Neu5Ac \rightarrow CMP-Neu5Gc), animal cells must harbor a pathway for degradation or elimination of Neu5Gc, to avoid accumulation of this endogenous molecule in excess. To date, however, a metabolic pathway for the turnover of Neu5Gc has not been reported. To address this question, human THP-1 cells were pulsed with exogenous Neu5Gc for 3 days and thereafter cultivated under Neu5Gc-free conditions to observe the fate of the incorporated Neu5Gc over time. Total cell lysates were prepared and analyzed by DMB-HPLC showing that almost 55% of total Sia was Neu5Gc after the initial pulse (1340.6 pmol of Neu5Gc and 1099.9 pmol of Neu5Ac, respectively). During the subsequent chase, the cells were found to lose loaded Neu5Gc over time (Fig. 2*A*). It is of course possible that cells simply excrete some of the loaded Neu5Gc in bound or free form as recently suggested by Inoue *et al.* (69). Unfortunately, high salt concentrations and a huge excess of Neu5Ac in the media did not allow reliable sensitive detection of small amounts of Neu5Gc in the media during the pulse-chase experiment. Regardless, evolution commonly shapes highly energy-efficient systems. Cells that have metabolic pathways to synthesize a certain structure commonly also harbor the enzymatic machinery to degrade and recycle it. It is an adjustable equilibrium carefully regulated by metabolic cross-talk. Therefore, the loss of Neu5Gc from loaded cells over time indicates that mammalian cells likely harbor an as yet unknown pathway for the turnover of Neu5Gc.

Conceivable Pathway for the Metabolic Turnover of Excess Neu5Gc in Mammalian Cells—Based on the well studied metabolism of *N*-acetylhexosamines in mammalian cells, we considered a pathway for degradation of excess Neu5Gc (Fig. 2*B*) involving the following four steps. (*a*) Conversion of

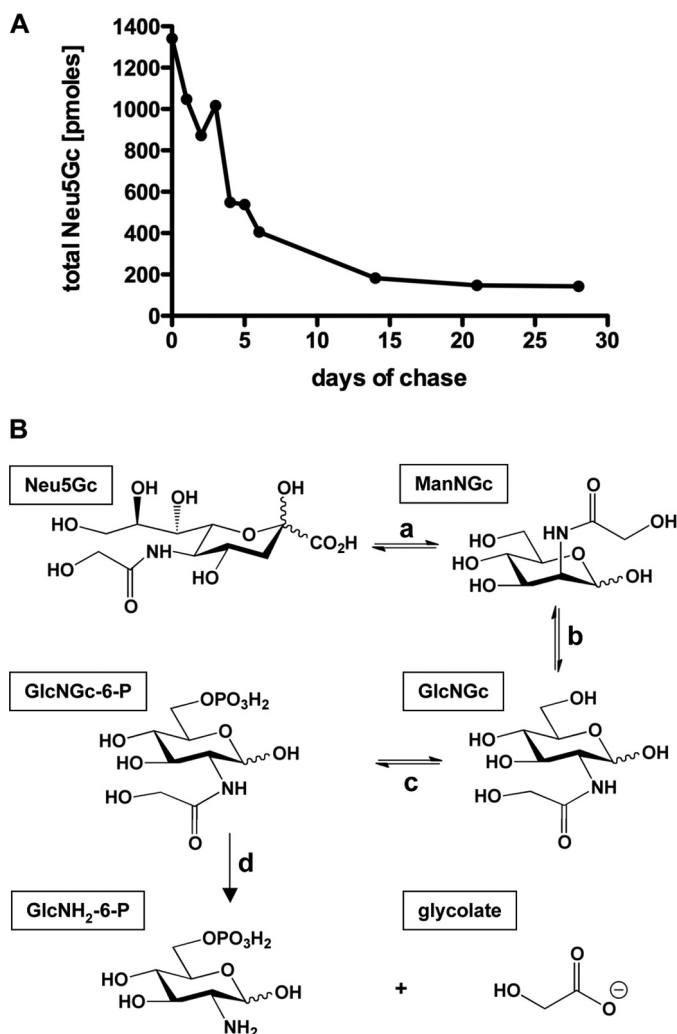


FIGURE 2. Elimination of Neu5Gc in Neu5Gc-loaded cells over time. A, human THP-1 cells were cultivated under Neu5Gc-free conditions using 5% human serum and confirmed to be devoid of detectable Neu5Gc. Thereafter, the feeding medium was supplemented with 5 mM Neu5Gc. After 3 days, the feeding media were removed, and cells were washed well, split equally into 10 aliquots, and grown under Neu5Gc-free conditions for up to 28 days. Additional media were added at day 7 and later as necessary. At different time points of the chase, all cells grown in one of the aliquots were harvested and pellets stored at -20°C . DMB-HPLC analysis was performed once all time points were collected. For DMB-HPLC analysis, total cell lysates were prepared, and the Neu5Gc contents were determined after mild acid hydrolysis. The total Neu5Gc content of each cell pellet was calculated and is depicted as pmol of Neu5Gc over time. B, proposed pathway for the metabolic turnover of excess Neu5Gc in mammalian cells. Neu5Gc is known to be a substrate for the pyruvate lyase, which results in the formation of ManNGc (a) (41, 42). Following epimerization from ManNGc toward GlcNGc, which is potentially catalyzed by the GlcNAc-2'-epimerase (b) (73, 74, 90), phosphorylation of GlcNGc in the 6 position might occur by action of the GlcNAc kinase (c) (75, 76) resulting in the formation of GlcNGc-6-P. Thereafter, the *N*-glycolyl group might be irreversibly removed from GlcNGc-6-P by the GlcNAc-6-P deacetylase (d) (76, 77), which would result in GlcNH₂-6-P, a precursor *e.g.* for glycolysis, and glycolate, a molecule able to enter the citric acid cycle via glyoxylate.

Neu5Gc into *N*-glycolylmannosamine (ManNGc) was catalyzed by the *N*-acetylneuraminic acid pyruvate-lyase (EC 4.1.3.3). The respective lyase enzymes from pig kidney and human erythrocytes have already been demonstrated to degrade Neu5Gc. Compared with the substrate Neu5Ac (100%), Neu5Gc was cleaved at relative rates of 47–65% by such enzymes (41, 42, 70–72). (b) Subsequent epimerization was from ManNGc toward *N*-glycolylglucosamine (GlcNGc),

which is potentially catalyzed by the GlcNAc 2'-epimerase (EC 5.1.3.8). Interestingly, the GlcNAc 2'-epimerase isolated from pig kidney has been mentioned previously to be able to interconvert ManNGc and GlcNGc (73). Moreover, GlcNAc 2'-epimerase was found to have a pronounced catabolic role with regard to the substrates ManNAc/GlcNAc, diverting metabolic flux away from sialic acids (74). (c) The next step would involve phosphorylation of GlcNGc in the 6 position by action of the GlcNAc kinase (EC 2.7.1.59) resulting in the formation of *N*-glycolylglucosamine 6-phosphate (GlcNGc-6-P) (75, 76). (d) We hypothesize that the *N*-glycolyl group can then be irreversibly removed from GlcNGc-6-P by the GlcNAc-6-P deacetylase (EC 3.5.1.25) similar to de-*N*-acetylation of GlcNAc-6-P (76, 77). This would result in the formation of the two common metabolites glucosamine 6-phosphate (GlcNH₂-6-P), a precursor, *e.g.* for glycolysis, and glycolate, a molecule able to enter the citric acid cycle.

Synthesis of Radiolabeled and Nonlabeled Compounds—To study the Neu5Gc-degrading pathway predicted above, radiolabeled and nonlabeled versions of all putative intermediates were prepared using chemical and enzymatic protocols. Briefly, nonlabeled *N*-glycolylated hexosamines were prepared by reaction of the 2-amino-2-deoxyhexosamine with acetoxyacetylchloride under basic aqueous conditions followed by purification using ion-exchange resin chromatography. Per-*O*-acetylated analogs were prepared using acetic anhydride under basic aqueous additions and isolated by drying under vacuum without further purification. Nonlabeled Neu5Gc was prepared as per a previously described protocol (55). With regard to the radiolabeled material, we first synthesized [³H]glycolic acid starting from glyoxylate and [³H]NaBH₄. The [³H]glycolic acid was then used to prepare [glycolyl-³H]ManNGc, [glycolyl-³H]GlcNGc, and [glycolyl-³H]GlcNGc-6-P, and finally [glycolyl-³H]Neu5Gc from [glycolyl-³H]ManNGc as described under “Experimental Procedures.” Thus, all compounds carry the radiolabel exclusively in the *N*-glycolyl group, which allows tracking the pathway. Next, a method was developed to separate all intermediates of the predicted pathway by HPLC using a PA-1 column under alkaline conditions (supplemental Fig. S2). Subsequently, the identity of all synthesized radiolabeled compounds was confirmed by HPLC, observing co-elution with their chemically well characterized, nonlabeled counterparts (data not shown). As glycolate cannot be detected by HPAEC-PAD due to the lack of ionizable hydroxyl groups, the identity of synthesized [³H]glycolic acid was confirmed by co-elution with commercial [¹⁴C]glycolic acid. The elution profile of a standard mixture containing [³H]ManNGc, [¹⁴C]GlcNGc, [³H]GlcNGc-6-P, [³H]glycolic acid, and [¹⁴C] glycolic acid confirms separation of all pathway intermediates (Fig. 3A).

Evidence for the Predicted Neu5Gc-degrading Pathway in Mouse Tissue Cytosolic Extracts—To study the predicted Neu5Gc-degrading pathway, a fresh cytosolic extract from mouse liver was prepared and incubated in the presence of the synthesized radiolabeled compounds described above. Subsequently, the reaction mixtures were analyzed by HPLC followed by scintillation counting to identify the reaction products (Fig. 3 and supplemental Fig. S2). Incubation of [³H]ManNGc in the presence of fresh cytosolic extract resulted in formation of

Metabolic Fate of *N*-Glycolylneuraminic Acid

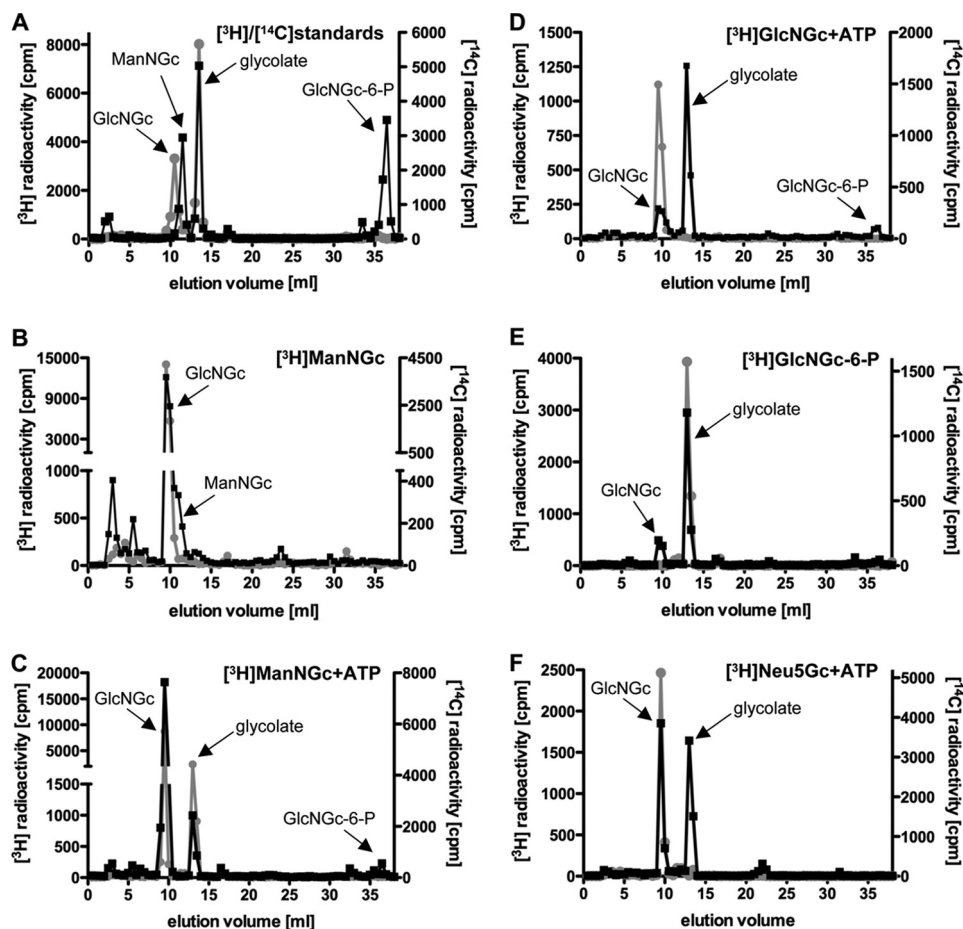


FIGURE 3. Evidence for the predicted Neu5Gc-degrading pathway in murine tissue cytosolic extracts. To study the putative degradative pathway of Neu5Gc, all predicted intermediates harboring a radiolabel in the *N*-glycolyl group were prepared. *A*, separation of [^3H]ManNGc, [^{14}C]GlcNGc, [^3H]GlcNGc-6-P, and [^3H]glycolate and commercially available [^{14}C]glycolate was achieved by HPLC under alkaline conditions using a PA-1 column. Fractions (0.5 ml) were collected, and radioactivity was determined by scintillation counting. The elution profile of [^3H] radioactivity refers to the left y axis (black symbols and line) and [^{14}C] radioactivity (gray symbols and line) is depicted on the right y axis. *B*, freshly prepared mouse liver cytosolic extracts were incubated with [^3H]ManNGc for 6 h at 37 °C. The reaction was quenched by addition of ethanol (70% final) and subsequent precipitation at -20 °C overnight. The supernatant was supplemented with [^{14}C]GlcNGc as an internal standard, followed by HPLC analysis and subsequent scintillation counting as described above. The elution profile reveals [^3H] radioactivity (black symbols and line) derived from the [^3H]ManNGc in the sample on the left y axis, and [^{14}C] radioactivity (gray symbols and line) from the internal standard is shown on the right y axis. *C*, freshly prepared mouse liver cytosolic extracts were incubated with [^3H]ManNGc for 6 h at 37 °C. To ensure the presence of ATP to allow the putative kinase reaction (GlcNGc \rightarrow GlcNGc-6-P), 5 mM ATP, 10 mM MgCl_2 , and additional lysate were added at 6 h, and the reaction mixture was incubated for another 6 h at 37 °C. Thereafter, the reaction mixture was analyzed and depicted as described for *B*. [^{14}C]GlcNGc and [^{14}C]glycolate were added as internal standards. Notably, the predicted pathway intermediate GlcNGc-6-P cannot be detected in this assay as the radiolabels are placed in the *N*-glycolyl groups exclusively. *D*, freshly prepared mouse liver cytosolic extracts were incubated with [^3H]GlcNGc in the presence of 5 mM ATP and 10 mM MgCl_2 for 6 h at 37 °C. The sample was worked up, analyzed, and presented as mentioned above in *B*. *E*, freshly prepared mouse liver cytosolic extracts were incubated with [^3H]GlcNGc-6-P for 6 h at 37 °C. The reaction mixture was analyzed and depicted as described in *B*. *F*, freshly prepared mouse liver cytosolic extracts were incubated with [^3H]Neu5Gc for 6 h at 37 °C. Thereafter, 5 mM ATP, 10 mM MgCl_2 , and additional lysate were added as described in *C*, and the reaction mixture was incubated for another 6 h at 37 °C. Thereafter, the reaction mixture was analyzed and depicted as described for *B*. The displayed data are representative of at least three independent experiments.

[^3H]GlcNGc, demonstrating the presence of the predicted GlcNAc 2'-epimerase activity in the tissue extracts (Fig. 3*B*). The almost complete conversion toward [^3H]GlcNGc is in line with the marked preferential catabolic properties of the GlcNAc 2'-epimerase enzyme described previously (74). The lack of further conversion toward GlcNGc-6-P and glycolate is likely explained by the absence of ATP, which is a required cofactor for the GlcNAc kinase to catalyze the 6-phosphorylation of GlcNGc. We assumed that unstable endogenous ATP from the fresh mouse liver might have degraded during the preparation of the cytosolic extracts. Indeed, incubation of [^3H]ManNGc in the presence of additional ATP resulted in formation of small amounts of [^3H]GlcNGc-6-P and [^3H]glycolate, but [^3H]GlcNGc remained by far the predominant product

(data not shown). Of note, GlcNH₂-6-P cannot be observed in this assay as it no longer carries the radiolabeled *N*-glycolyl moiety. We assumed that the GlcNAc kinase activity might not be completely preserved in the reaction mixture by the time enough [^3H]GlcNGc had formed. To test this, [^3H]ManNGc was first preincubated with cytosolic extracts alone before ATP and additional fresh tissue extract were added. Indeed, significant amounts of [^3H]glycolate were now detectable among the reaction products (Fig. 3*C*). Conversion toward [^3H]glycolate was even more pronounced when [^3H]GlcNGc was incubated directly with cytosolic extracts in the presence of ATP (Fig. 3*D*), indicating that the GlcNAc kinase was indeed unstable in the reaction conditions. In this experiment, [^3H]glycolate represents the main reaction product (Fig. 3*D*), and the predicted

intermediate GlcNGc-6-P was detectable at significantly lower levels among the reaction products. To test if glycolate is indeed released from GlcNGc-6-P, [^3H]GlcNGc-6-P was directly incubated in the presence of cytosolic extracts. As predicted, [^3H]glycolate represents the main product (Fig. 3E), indicating that the *N*-glycolyl group can be irreversibly removed by action of the GlcNAc-6-P deacetylase enzyme. The occurrence of GlcNGc among the reaction products is likely explained by nonspecific phosphatases known to be present in tissue extracts (Fig. 3E). In line with the almost complete conversion of [^3H]ManNGc to [^3H]GlcNGc (Fig. 3B), incubation of [^3H]Neu5Gc with cytosolic extracts in the absence of ATP only resulted in formation of [^3H]GlcNGc (data not shown). However, when [^3H]Neu5Gc was first preincubated with cytosolic extracts before the reaction mixture was supplemented with ATP and additional fresh cytosolic extracts, significant release of [^3H]glycolate was observed (Fig. 3F). This provides strong evidence that the predicted Neu5Gc-degrading pathway was indeed qualified to eliminate excess Neu5Gc from mammalian cells, and all enzymes involved tolerate substrates with an *N*-glycolyl group, at least to some extent. In addition, no direct de-*N*-glycolylation of either [^3H]Neu5Gc or its immediate breakdown product [^3H]ManNGc was observed when incubated with mouse liver cytosolic extracts (Fig. 3B), suggesting that no such unknown direct enzyme activity exists.

Of course, this somewhat artificial system using cytosolic extracts from murine liver is not meant to represent the actual kinetics of the Neu5Gc-degrading pathway as careful cellular control of the metabolic flux cannot be assumed to be preserved. Moreover, the obvious lack of compartmentalization in such cytosolic extracts of course hinders activation of Neu5Gc by the CMP-sialic acid synthetase, which would predominantly take place in the nucleus (78, 79). The absence of this alternative metabolic route likely drives the Neu5Gc-degrading pathway in the cytosolic extracts.

Enzymatic Phosphorylation of GlcNGc to Generate GlcNGc-6-P Is Catalyzed by the GlcNAc Kinase—Conversion of Neu5Gc to ManNGc catalyzed by mammalian *N*-acetylneuraminic pyruvate-lyases has been conclusively demonstrated previously using the respective lyase enzymes from pig kidney and human erythrocytes (41, 42, 70–72). The GlcNAc 2'-epimerase from pig kidney has also been mentioned previously to catalyze interconversion of ManNGc and GlcNGc (73). Moreover, almost complete conversion of [^3H]ManNGc toward [^3H]GlcNGc was observed in murine tissue cytosolic extracts as described above, and this finding is in line with the pronounced catabolic role suggested for the GlcNAc 2'-epimerase to divert metabolic flux away from sialic acids (74). Taken together, the first two steps of the predicted Neu5Gc-degrading pathway have been conclusively demonstrated to take place. However, the predicted pathway intermediate GlcNGc-6-P potentially resulting from subsequent phosphorylation of GlcNGc was not observed in significant amounts by studying murine liver cytosolic extracts (Fig. 3, C, D, and F). Thus, we next turned to prove the existence of this proposed degradative step using the recombinant enzyme. Therefore, human *NAGK* gene encoding the GlcNAc kinase was cloned into pGEX-2T vector, recombinantly expressed in *E. coli* BL21(DE3), and purified via an N-terminal

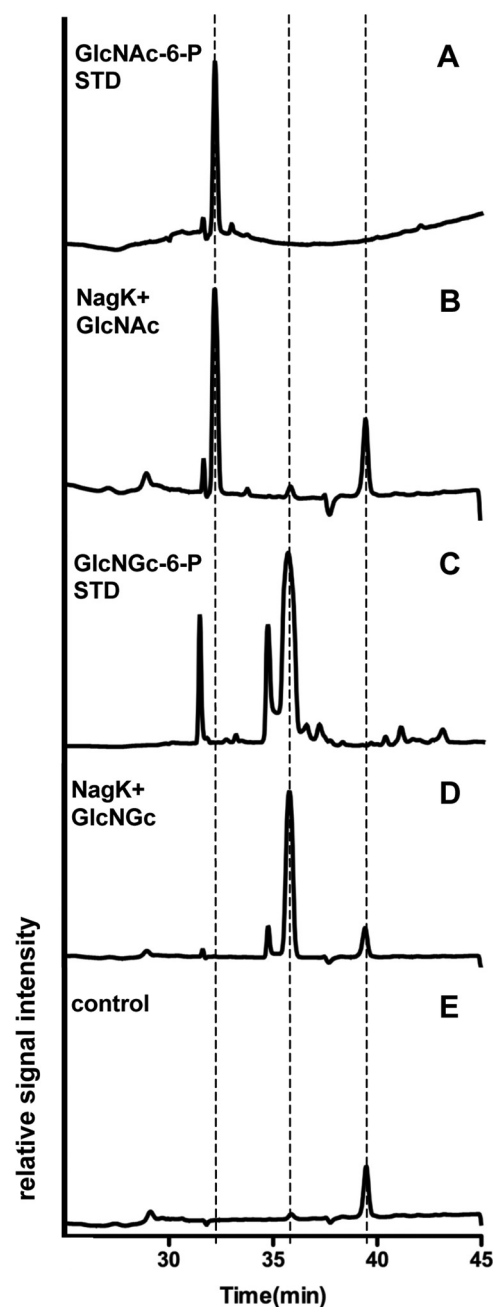


FIGURE 4. Purified recombinant human GlcNAc kinase NagK phosphorylates GlcNGc. Purified recombinant human GlcNAc kinase NagK was incubated with either 1 mM commercially available GlcNAc or 1 mM synthesized GlcNGc in the presence of 50 mM Tris-HCl pH 7.5, 10 mM MgCl_2 , 5 mM ATP, and 5 mM DTT for 1 h at 37 °C. Reactions were quenched with ethanol (70% final), and the protein was precipitated overnight. The filtered supernatants were analyzed by HPAEC-PAD HPLC under alkaline conditions using a PA-1 column. *A*, 1 μg of GlcNAc-6-P standard. *B*, NagK reaction mixture with GlcNAc as the substrate. *C*, 1 μg of GlcNGc-6-P standard. *D*, NagK reaction mixture with GlcNGc as the substrate. *E*, control reaction lacking substrates to determine the background arising from the NagK enzyme preparation.

GST fusion part as described previously (43, 44). An activity assay was set up (43) with the isolated recombinant GlcNAc kinase and either GlcNAc or synthesized GlcNGc as substrates. The reaction mixture was then analyzed by HPLC with HPAEC-PAD as described above (supplemental Fig. S2). Conversion of GlcNAc into GlcNAc-6-P confirmed that recombinant human GlcNAc kinase was isolated in an active form (Fig.

Metabolic Fate of N-Glycolylneuraminic Acid

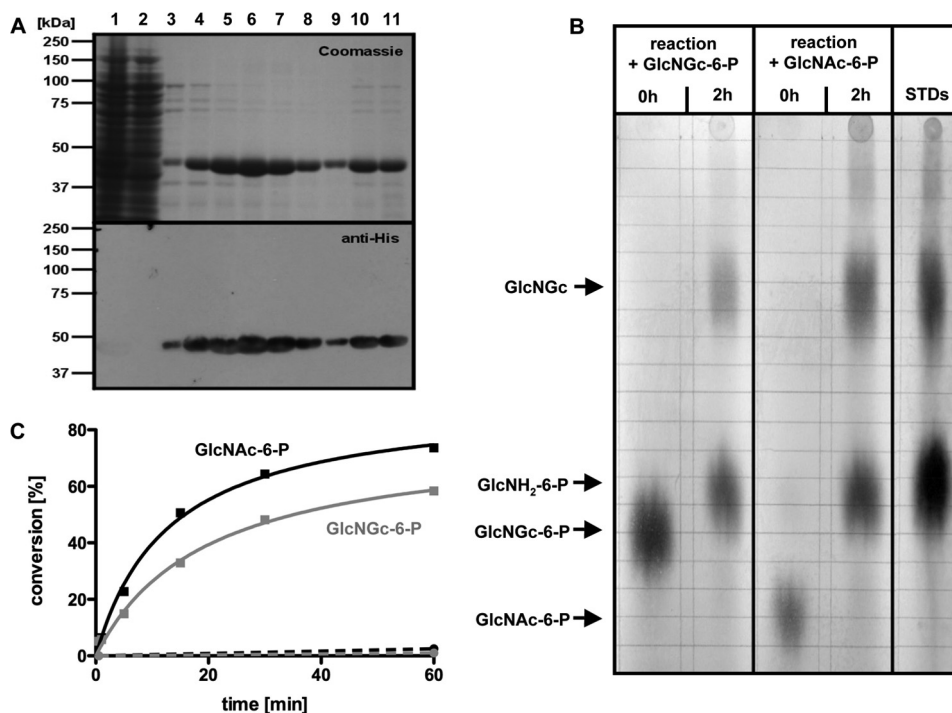


FIGURE 5. Purified recombinant human GlcNAc-6-P deacetylase was purified and shown to remove the N-glycolyl group of GlcNGc-6-P. *A*, human GlcNAc-6-P deacetylase was cloned into pET22b vector, expressed in *E. coli* BL21(DE3) carrying a C-terminal hexahistidine tag, and isolated using immobilized metal affinity chromatography followed by dialysis. Steps of the purification process were analyzed by 10% SDS-PAGE followed by Coomassie staining (*upper panel*) or Western blot detection using anti-His antibody (*lower panel*). Shown are aliquots of the bacterial lysate (*lane 1*), run-through (*lane 2*), wash fraction (*lane 3*), enzyme-containing fractions eluted from the immobilized metal affinity chromatography column (*lanes 4–9*), and the pool of enzyme-containing fractions before (*lane 10*) and after (*lane 11*) dialysis. *B*, activity assays to demonstrate enzymatic activity of the purified recombinant human GlcNAc-6-P deacetylase were set up with either commercially available GlcNAc-6-P or synthesized GlcNGc-6-P as substrates. Aliquots of the reaction mixtures at 0 and 120 min were analyzed by descending paper chromatography followed by silver staining. As a standard (STD), the expected reaction product GlcNH₂-6-P was analyzed as well as GlcNGc. *C*, purified recombinant human GlcNAc-6-P deacetylase was incubated with either 2 mM commercial GlcNAc-6-P or ~2 mM synthesized GlcNGc-6-P in the presence of 25 mM Tris-HCl pH 7.5, and 1 mM DTT at 37 °C. At different time points, aliquots were removed; the enzymatic reaction was quenched by addition of ethanol (70% final), and the protein was precipitated overnight. The supernatants were dried down, resuspended in water, and analyzed by HPAEC-PAD HPLC under alkaline conditions using a PA-1 column. The areas under the substrate and product peaks were determined, and the conversion into GlcNH₂-6-P was calculated for all time points. The *graph* represents the conversion of the substrates, GlcNAc-6-P (*black symbols and line*) and GlcNGc-6-P (*gray symbols and line*), into the product GlcNH₂-6-P over time in percent. To control for nonenzymatic decay of the substrates over time, equivalent reactions were set up using heat-inactivated enzyme. No detectable decomposition of the substrates was found when incubating GlcNAc-6-P (*black dotted line*) or GlcNGc-6-P (*gray dotted line*).

4, *A* and *B*). Moreover, recombinant human GlcNAc kinase also acted on GlcNGc, which resulted in the formation of GlcNGc-6-P as predicted (Fig. 4, *C* and *D*) clearly demonstrating that human GlcNAc kinase tolerates the N-glycolyl group. The low abundance of the pathway intermediate [³H]GlcNGc-6-P in the study using tissue extracts may thus be explained by metabolic equilibrium, *i.e.* the irreversible nature of the following de-N-glycolylation reaction; but this does not necessarily reflect the situation *in vivo*.

Human GlcNAc-6-P Deacetylase Removes the N-glycolyl Group of GlcNGc-6-P—The final step of the proposed Neu5Gc-degrading pathway involves irreversible de-N-glycolylation of GlcNGc-6-P to yield glucosamine 6-phosphate (which could be further metabolized to fructose-6-P and glucose-6-P to enter glycolysis) and glycolate (which can enter the citric acid cycle via glyoxylate). Although release of [³H]glycolate was observed when murine tissue extracts were incubated with [³H]Neu5Gc, [³H]ManNGc, [³H]GlcNGc, or [³H]GlcNGc-6-P (Fig. 3, *C–F*), simple nonenzymatic breakdown cannot yet be unambiguously excluded. Thus, we next aimed to prove that the predicted GlcNAc-6-P deacetylase enzyme is required for this degradative step. Therefore, the

human *AMDHD2* gene predicted to encode GlcNAc-6-P deacetylase was cloned into a modified pET22b vector, expressed in *E. coli* BL21(DE3), and purified via the C-terminal hexahistidine (His₆) tag using immobilized metal affinity chromatography followed by dialysis. For the first time, we report recombinant expression and purification of human GlcNAc-6-P deacetylase in high yield (38.1 mg/liter) with only minor impurities (Fig. 5*A*). To confirm that the isolated enzyme is functional, activity assays were set up using either GlcNAc-6-P or GlcNGc-6-P as substrates. At first, reaction products were separated by descending paper chromatography, and the sugars were subsequently visualized by silver staining. Enzymatic activity was observed toward both substrates demonstrated by the occurrence of a shifted band, which co-migrates with the expected reaction product GlcNH₂-6-P (Fig. 5*B*). This result confirms that active recombinant human GlcNAc-6-P deacetylase was purified. Activity of isolated GlcNAc-6-P deacetylase toward GlcNAc-6-P and GlcNGc-6-P was further evaluated in an additional activity assay. To control for nonenzymatic decay of the substrates over time, equivalent reactions were set up using heat-inactivated enzyme. The reaction products were analyzed at different time points by HPLC

using HPAEC-PAD, and the areas under the substrate and product peaks were determined to calculate conversion into GlcNH₂-6-P at all time points (Fig. 5C). Enzymatic activity of the recombinant human GlcNAc-6-P deacetylase was observed toward both tested substrates. Although reactivity toward GlcNGc-6-P appears to be slightly lower as compared with GlcNAc-6-P, both reactions occur in the same range clearly suggesting that the predicted last step of the Neu5Gc-degrading pathway is to occur *in vivo*.

Proposed Neu5Gc-degrading Pathway Occurs in Human Cells—To further prove that the predicted Neu5Gc-degrading pathway actually occurs *in vivo*, the culturing media of human THP-I cells was supplemented with [³H]Neu5Gc, [³H]ManNGc, or [³H]GlcNGc. After labeling, cells were harvested; the lysates were cleaned up by ethanol precipitation, and a compositional analysis of the subsequent supernatant was performed by HPLC followed by scintillation counting. In general, uptake of such radiolabeled compounds with their low molarities into the cells was very poor, which is likely due to the lack of specific transporters in the cell membrane. Hence, after feeding cells with [³H]Neu5Gc, no significant radioactive signals of breakdown products were detectable (data not shown). The extremely low uptake observed for [³H]Neu5Gc might have been worsened by the high concentration of competing Neu5Ac in the culture media derived from the 5% human serum supplement. However, detectable amounts of [³H]ManNGc were taken up by the cells, and subsequent analysis by HPLC revealed that THP-I cells converted [³H]ManNGc into [³H]GlcNGc and [³H]glycolate, respectively (Fig. 6A). Even better uptake was observed when cells were incubated with [³H]GlcNGc. HPLC analysis demonstrated that human THP-I cells partially converted [³H]GlcNGc into [³H]GlcNGc-6-P and [³H]glycolate (Fig. 6B). Moreover, even small amounts of [³H]ManNGc were detectable among the products (Fig. 6B), highlighting once more the pronounced catabolic function of the GlcNAc 2'-epimerase. In light of the already well described ability of human erythrocytes to convert Neu5Gc into ManNGc (41), the above results clearly demonstrate that the predicted Neu5Gc-degrading pathway takes place in human cells. In general, results from cell feedings varied greatly between experiments with regard to the efficiency of uptake and the ratios of the products. This likely suggests that the metabolic state of the cells impacts uptake, regulation of the Neu5Gc-degrading pathway, and its interplay with cellular metabolism.

Predicted Neu5Gc-degrading Pathway Is Only Partially Reversible—The GlcNAc-6-P deacetylase reaction is not reversible, and our earlier finding that exogenously added glycolate in high amounts does not yield *de novo* biosynthesis of Neu5Gc indicated that glycolyl groups cannot be added back to GlcNH₂-6-P. However, the other steps of the degradative pathway are potentially reversible. The human sialate pyruvate-lyase has already been demonstrated to cleave Neu5Gc at ~60% of the rate obtained for Neu5Ac (41), and cultured rodent neural cells have been demonstrated to efficiently incorporate per-O-acetylated ManNGc (per-O-acetyl-ManNGc) from the feeding media and convert it to Neu5Gc (80). Peracetylation has previously been shown to greatly enhance uptake of carbohy-

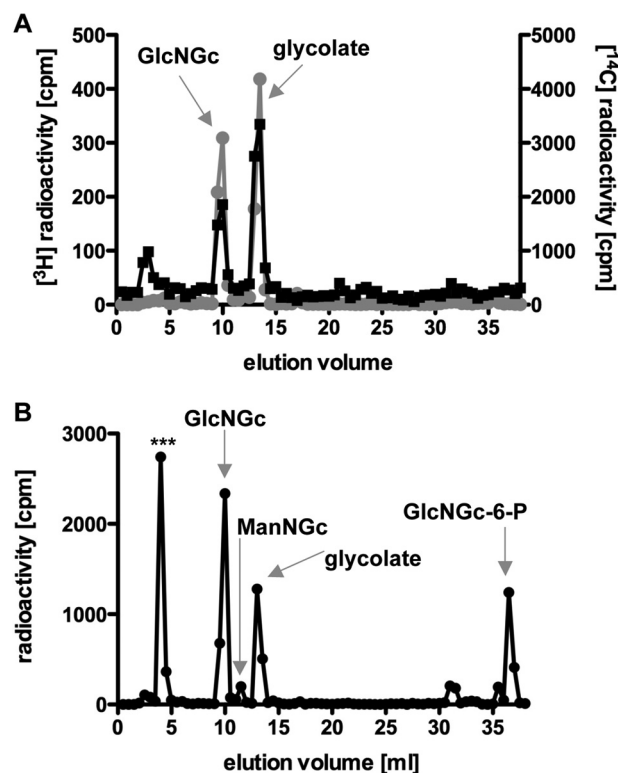


FIGURE 6. Proposed degradative pathway occurs in human cells. Human THP-I cells were cultivated under Neu5Gc-free conditions using 5% human serum. Thereafter, the culture medium was supplemented with either [³H]ManNGc or [³H]GlcNGc. After 3 days, the feeding medium was removed, and the cells were washed intensively with PBS. Subsequently, the cell pellets were resuspended in hypotonic 10 mM Tris-HCl pH 7.5, and lysed by repetitive freeze-thaw. Ethanol was added to a final concentration of 70%, and precipitation occurred at -20°C overnight. The supernatant was supplemented with internal standards and subsequently analyzed by HPLC under alkaline conditions using a PA-1 column. Fractions (0.5 ml) were collected, and radioactivity was determined by scintillation counting. *A*, THP-I cells fed with [³H]ManNGc were prepared and analyzed as described above. [¹⁴C]GlcNGc and [¹⁴C]glycolate were added as internal standards prior to HPLC analysis. The elution profile reveals [³H] radioactivity (black symbols and line) derived from the [³H]ManNGc in the sample on the left y axis, and [¹⁴C] radioactivity (gray symbols and line) from the internal standards is shown on the right y axis. *B*, THP-I cells fed with [³H]GlcNGc were treated as described above. [³H]Mannose (peak marked ***) was added as internal standard prior to HPLC analysis.

drates in cells (81) and increased conversion of ManNGc into Neu5Gc up to 100-fold (80). To further investigate the reversibility of the Neu5Gc-degrading pathway, ManNGc (55), GlcNGc, per-O-acetyl-ManNGc, and per-O-acetyl-GlcNGc (Fig. 7A) were synthesized and used for feeding experiments of THP-I cells and *Cmah*^{-/-} fibroblasts (Fig. 7B). Loaded cells were analyzed by flow cytometry using anti-Neu5Gc IgY (25). In keeping with previous reports using other cell types, the CMAH-deficient cells used in this study were able to convert ManNGc or per-O-acetyl-ManNGc into Neu5Gc, which was incorporated into cell-surface glycoconjugates (Fig. 7B). Interestingly, *Cmah*^{-/-} fibroblasts and THP-I cells were also able to use GlcNGc as a precursor for Neu5Gc biosynthesis, potentially via epimerization to ManNGc. Although 100 μM GlcNGc in the feeding media was insufficient to achieve detectable amounts of cell-surface exposed Neu5Gc, 100 μM per-O-acetyl-GlcNGc yielded a low but significant signal (Fig. 7C). However, increasing the GlcNGc concentration in the feeding media to 10 mM

Metabolic Fate of N-Glycolylneuraminic Acid

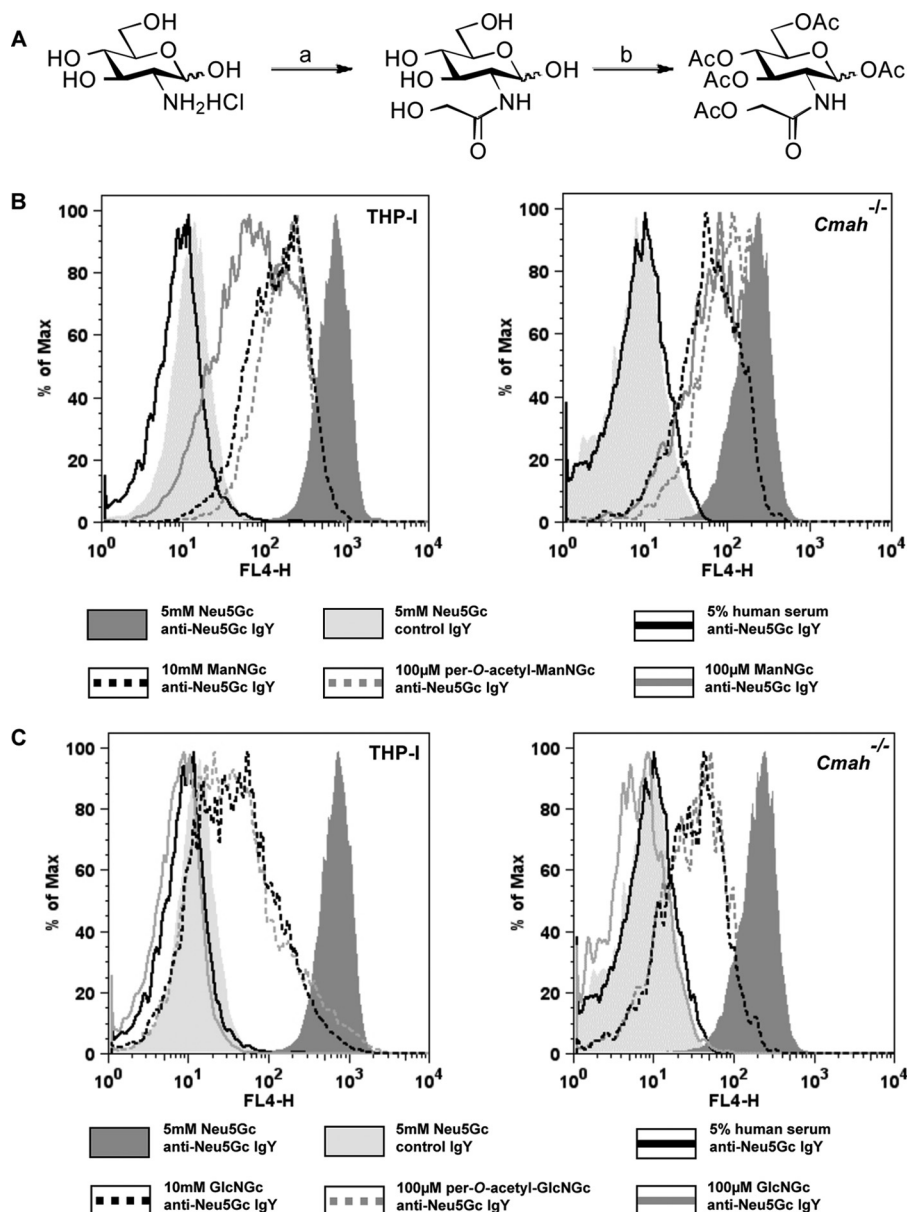


FIGURE 7. Proposed Neu5Gc-degrading pathway is partially reversible. *A*, synthesis of GlcNGc and peracetylated GlcNGc from a commercial source of glucosamine. *a*, acetoxyacetyl chloride and aqueous sodium bicarbonate (yield = 94%). *b*, pyridine and acetic anhydride (yield = 90%). *B*, human THP-I cells and murine *Cmah*^{-/-} fibroblasts were cultivated under Neu5Gc-free conditions using 5% human serum. Thereafter, the feeding media were supplemented with either 5 mM Neu5Gc (positive control; shaded dark gray) or synthesized ManNGc and GlcNGc derivatives. In parallel, cells were kept in 5% human serum without feeding (negative control; black line). After 3 days of feeding, cells were harvested and analyzed by flow cytometry using anti-Neu5Gc IgY (25) for sensitive detection of cell-surface glycosidically bound Neu5Gc. As an additional negative control, cells fed 5 mM Neu5Gc were also stained with control chicken IgY antibody (control IgY; shaded light gray). Histograms of THP-I cells (left panel) and *Cmah*^{-/-} fibroblasts (right panel) are shown. Cells were fed either 100 μ M ManNGc (gray line), 10 mM ManNGc (dotted black line), or 100 μ M per-*O*-acetylated ManNGc (per-*O*-acetyl-ManNGc) in addition to the controls described above. *C*, flow cytometry analysis of THP-I cells (left panel) and *Cmah*^{-/-} fibroblasts (right panel). Cells were incubated with either 100 μ M GlcNGc (gray line), 10 mM GlcNGc (dotted black line), or 100 μ M peracetylated GlcNGc (per-*O*-acetyl-GlcNGc) in the feeding media. Experiments were done in parallel with the control feedings explained above.

resulted in comparable amounts of cell-surface Neu5Gc, confirming that peracetylation significantly enhances uptake and utilization of GlcNGc (Fig. 7C). The significantly lower levels of detectable cell-surface Neu5Gc after feeding with GlcNGc, compared with feeding with ManNGc, are in line with previous reports that the GlcNAc 2'-epimerase potentially catalyzing inter-conversion of ManNGc and GlcNGc has a predominantly catabolic function (74).

Conclusions and Future Perspectives—In this study, we demonstrate that mammalian cells harbor the enzymatic machinery

to degrade Neu5Gc by sequential conversion into ManNGc, GlcNGc, and GlcNGc-6-P. The final de-*N*-glycolylation step results in formation of the ubiquitous well described metabolites GlcNH₂-6-P (which can enter glycolysis by further conversion to fructose-6-P and glucose-6-P) and glycolate (which can enter the citric acid cycle via glyoxylate). This proposed Neu5Gc-degrading pathway was shown to occur to a significant extent in CMAH-deficient human THP-I cells and wild-type murine liver cytosolic extracts suggesting that the predicted pathway is likely occurring in mammals *in vivo*. Although we

demonstrate the presence of this Neu5Gc-degrading metabolic pathway, which may regulate Neu5Gc-levels in mammalian cells, we do not exclude involvement of additional pathways for elimination of Neu5Gc from cells such as excretion of Neu5Gc-containing sialylated glycoconjugates (69) or less likely simple excretion of the monosaccharide.

The identification of a Neu5Gc-degrading pathway in mammalian cells may help explain why Neu5Gc in humans only accumulates in cells close to the bloodstream, which represents the supply route of exogenous Neu5Gc in the absence of CMAH activity (likely resorbed from the gut and originating from foods (82)). If simple secretion of Neu5Gc in free or bound form were to be the major routes for mammalian cells to eliminate excess Neu5Gc, equal distribution of Neu5Gc expression throughout human tissues would likely be the consequence over time, due to continuous recycling of excreted Neu5Gc by pinocytosis. However, this does not reflect the situation found in humans (26). By contrast, Neu5Gc expression in humans and Neu5Gc-loaded *Cmah*^{-/-} mice is detectable in normal tissues lining the blood vessels or in close proximity to blood vessels (25, 26, 28) suggesting that exogenously derived Neu5Gc enters an equilibrium between uptake into cells depending on direct supply and subsequent turnover, including irreversible degradation. As growing tumors are highly vascularized and characterized by high metabolism involving significantly increased macropinocytosis (83–85), these malignant cells are likely taking up more circulating Neu5Gc as compared with surrounding normal human cells at a time. Also, hypoxia up-regulates gene expression of the lysosomal sialin transporter, which releases free sialic acids into the cytosol (86). Together such mechanisms likely explain why Neu5Gc was suggested to be a tumor-specific antigen in the past when less sensitive detection methods did not yet reveal its lower abundance on normal human cells (24, 26, 64).

Further studies are currently ongoing to investigate the underlying kinetics of Neu5Gc incorporation and turnover using the *Cmah*^{-/-} mouse model (18). These studies should reveal if Neu5Gc accumulation in humans represents a snapshot of the last meals (fast turnover) or reflects dietary preferences over the recent past (slow turnover). However, in the face of the described Neu5Gc-degrading pathway, simple switching to a Neu5Gc-free diet should likely eliminate already accumulated Neu5Gc from the human body over time. Thus, adjusting the diet may further support current treatment of diseases involving chronic inflammation, which may be aggravated by xenosialitis (reaction of human anti-Neu5Gc antibodies with the non-human xeno-autoantigen Neu5Gc being expressed) (31). An alternative approach involves eliminating Neu5Gc by metabolic competition with Neu5Ac (87). In addition, epidemiological studies comprising analysis of biopsy samples and tumor sections from individuals on a Standard Western Diet (which includes consumption of Neu5Gc-rich foods such as red meats), vegetarians (a diet that seem to be low in Neu5Gc), and vegans (so far assumed to have a Neu5Gc-free diet) may reveal a more detailed picture. These studies will likely also benefit from the currently ongoing comprehensive analyses on the Neu5Gc content of food products and the results in the accompanying paper (28) regarding the mechanisms of Neu5Gc

uptake from the gastrointestinal tract. Additional companion papers report on the incorporation of GlcNGc in O-linkage into nucleocytoplasmic proteins (88) and the tolerance of metabolic pathways for N-glycolylhexosamines (89).

Acknowledgments—We thank Bradley Hayes, Natasha Naidu, and Biswa Choudhury from University of California San Diego, Glycotechnology Core Resource for their help with the development of some methods for this study. We also thank Xi Chen for kindly providing the plasmid for recombinant expression of N-acetylneuraminic pyruvate-lyase from *P. multocida*.

REFERENCES

- Schauer, R. (1978) Characterization of sialic acids. *Methods Enzymol.* **50**, 64–89
- Troy, F. A. (1992) Polysialylation. From bacteria to brains. *Glycobiology* **2**, 5–23
- Varki, A., and Schauer, R. (2009) in *Essentials of Glycobiology* (Varki, A., Cummings, R. D., Esko, J. D., Freeze, H. H., Stanley, P., Bertozzi, C. R., Hart, G. W., and Etzler, M. E., eds) pp. 199–218, Cold Spring Harbor Laboratory Press, Cold Spring Harbor, NY
- Cohen, M., and Varki, A. (2010) The sialome. Far more than the sum of its parts. *OMICS* **14**, 455–464
- Harduin-Lepers, A., Vallejo-Ruiz, V., Krzewinski-Recchi, M. A., Samyn-Petit, B., Julien, S., and Delannoy, P. (2001) The human sialyltransferase family. *Biochimie* **83**, 727–737
- Shaw, L., and Schauer, R. (1988) The biosynthesis of N-glycolylneuraminic acid occurs by hydroxylation of the CMP-glycoside of N-acetylneuraminic acid. *Biol. Chem. Hoppe-Seyler* **369**, 477–486
- Kozutsumi, Y., Kawano, T., Yamakawa, T., and Suzuki, A. (1990) Participation of cytochrome *b*₅ in CMP-N-acetylneuraminic acid hydroxylation in mouse liver cytosol. *J. Biochem.* **108**, 704–706
- Shaw, L., Schneckenburger, P., Carlsen, J., Christiansen, K., and Schauer, R. (1992) Mouse liver cytidine-5'-monophosphate-N-acetylneuraminic acid hydroxylase. Catalytic function and regulation. *Eur. J. Biochem.* **206**, 269–277
- Kawano, T., Kozutsumi, Y., Takematsu, H., Kawasaki, T., and Suzuki, A. (1993) Regulation of biosynthesis of N-glycolylneuraminic acid-containing glycoconjugates. Characterization of factors required for NADH-dependent cytidine 5'-monophosphate-N-acetylneuraminic acid hydroxylation. *Glycoconj. J.* **10**, 109–115
- Shaw, L., Schneckenburger, P., Schlenzka, W., Carlsen, J., Christiansen, K., Jürgensen, D., and Schauer, R. (1994) CMP-N-acetylneuraminic acid hydroxylase from mouse liver and pig submandibular glands. Interaction with membrane-bound and soluble cytochrome *b*₅-dependent electron transport chains. *Eur. J. Biochem.* **219**, 1001–1011
- Takematsu, H., Kawano, T., Koyama, S., Kozutsumi, Y., Suzuki, A., and Kawasaki, T. (1994) Reaction mechanism underlying CMP-N-acetylneuraminic acid hydroxylation in mouse liver. Formation of a ternary complex of cytochrome *b*₅, CMP-N-acetylneuraminic acid, and a hydroxylation enzyme. *J. Biochem.* **115**, 381–386
- Kawano, T., Koyama, S., Takematsu, H., Kozutsumi, Y., Kawasaki, H., Kawashima, S., Kawasaki, T., and Suzuki, A. (1995) Molecular cloning of cytidine monophosphate-N-acetylneuraminic acid hydroxylase. Regulation of species- and tissue-specific expression of N-glycolylneuraminic acid. *J. Biol. Chem.* **270**, 16458–16463
- Schlenzka, W., Shaw, L., Kelm, S., Schmidt, C. L., Bill, E., Trautwein, A. X., Lottspeich, F., and Schauer, R. (1996) CMP-N-acetylneuraminic acid hydroxylase. The first cytosolic Rieske iron-sulfur protein to be described in Eukarya. *FEBS Lett.* **385**, 197–200
- Chou, H. H., Takematsu, H., Diaz, S., Iber, J., Nickerson, E., Wright, K. L., Muchmore, E. A., Nelson, D. L., Warren, S. T., and Varki, A. (1998) A mutation in human CMP-sialic acid hydroxylase occurred after the Homo-Pan divergence. *Proc. Natl. Acad. Sci. U.S.A.* **95**, 11751–11756
- Irie, A., Koyama, S., Kozutsumi, Y., Kawasaki, T., and Suzuki, A. (1998)

- The molecular basis for the absence of *N*-glycolylneuraminic acid in humans. *J. Biol. Chem.* **273**, 15866–15871
16. Hayakawa, T., Aki, I., Varki, A., Satta, Y., and Takahata, N. (2006) Fixation of the human-specific CMP-*N*-acetylneuraminic acid hydroxylase pseudogene and implications of haplotype diversity for human evolution. *Genetics* **172**, 1139–1146
 17. Varki, A. (2001) *N*-Glycolylneuraminic acid deficiency in humans. *Biochimie* **83**, 615–622
 18. Hedlund, M., Tangvoranuntakul, P., Takematsu, H., Long, J. M., Housley, G. D., Kozutsumi, Y., Suzuki, A., Wynshaw-Boris, A., Ryan, A. F., Gallo, R. L., Varki, N., and Varki, A. (2007) *N*-Glycolylneuraminic acid deficiency in mice. Implications for human biology and evolution. *Mol. Cell. Biol.* **27**, 4340–4346
 19. Higashi, H., Hirabayashi, Y., Fukui, Y., Naiki, M., Matsumoto, M., Ueda, S., and Kato, S. (1985) Characterization of *N*-glycolylneuraminic acid-containing gangliosides as tumor-associated Hanganutziu-Deicher antigen in human colon cancer. *Cancer Res.* **45**, 3796–3802
 20. Miyoshi, I., Higashi, H., Hirabayashi, Y., Kato, S., and Naiki, M. (1986) Detection of 4-*O*-acetyl-*N*-glycolylneuraminyl lactosylceramide as one of tumor-associated antigens in human colon cancer tissues by specific antibody. *Mol. Immunol.* **23**, 631–638
 21. Hirabayashi, Y., Higashi, H., Kato, S., Taniguchi, M., and Matsumoto, M. (1987) Occurrence of tumor-associated ganglioside antigens with Hanganutziu-Deicher antigenic activity on human melanomas. *Jpn. J. Cancer Res.* **78**, 614–620
 22. Kawachi, S., Saida, T., Uhara, H., Uemura, K., Taketomi, T., and Kano, K. (1988) Heterophile Hanganutziu-Deicher antigen in ganglioside fractions of human melanoma tissues. *Int. Arch. Allergy Appl. Immunol.* **85**, 381–383
 23. Devine, P. L., Clark, B. A., Birrell, G. W., Layton, G. T., Ward, B. G., Alewood, P. F., and McKenzie, I. F. (1991) The breast tumor-associated epitope defined by monoclonal antibody 3E1.2 is an *O*-linked mucin carbohydrate containing *N*-glycolylneuraminic acid. *Cancer Res.* **51**, 5826–5836
 24. Malykh, Y. N., Schauer, R., and Shaw, L. (2001) *N*-Glycolylneuraminic acid in human tumors. *Biochimie* **83**, 623–634
 25. Diaz, S. L., Padler-Karavani, V., Ghaderi, D., Hurtado-Ziola, N., Yu, H., Chen, X., Brinkman-Van der Linden, E. C., Varki, A., and Varki, N. M. (2009) Sensitive and specific detection of the non-human sialic acid *N*-glycolylneuraminic acid in human tissues and biotherapeutic products. *PLoS ONE* **4**, e4241
 26. Tangvoranuntakul, P., Gagneux, P., Diaz, S., Bardor, M., Varki, N., Varki, A., and Muchmore, E. (2003) Human uptake and incorporation of an immunogenic nonhuman dietary sialic acid. *Proc. Natl. Acad. Sci. U.S.A.* **100**, 12045–12050
 27. Bardor, M., Nguyen, D. H., Diaz, S., and Varki, A. (2005) Mechanism of uptake and incorporation of the non-human sialic acid *N*-glycolylneuraminic acid into human cells. *J. Biol. Chem.* **280**, 4228–4237
 28. Banda, K., Gregg, C. J., Chow, R., Varki, N., and Varki, A. (2012) Metabolism of vertebrate amino sugars with *N*-glycolyl groups. Mechanisms underlying gastrointestinal incorporation of the non-human sialic acid xeno-autoantigen *N*-glycolylneuraminic acid. *J. Biol. Chem.* **287**, 28852–28864
 29. Padler-Karavani, V., Yu, H., Cao, H., Chokhawala, H., Karp, F., Varki, N., Chen, X., and Varki, A. (2008) Diversity in specificity, abundance, and composition of anti-Neu5Gc antibodies in normal humans: potential implications for disease. *Glycobiology* **18**, 818–830
 30. Nguyen, D. H., Tangvoranuntakul, P., and Varki, A. (2005) Effects of natural human antibodies against a nonhuman sialic acid that metabolically incorporates into activated and malignant immune cells. *J. Immunol.* **175**, 228–236
 31. Varki, N. M., Strobert, E., Dick, E. J., Jr., Benirschke, K., and Varki, A. (2011) Biomedical differences between human and nonhuman hominids. Potential roles for uniquely human aspects of sialic acid biology. *Annu. Rev. Pathol.* **6**, 365–393
 32. Padler-Karavani, V., Hurtado-Ziola, N., Pu, M., Yu, H., Huang, S., Muthana, S., Chokhawala, H. A., Cao, H., Secrest, P., Friedmann-Morvinski, D., Singer, O., Ghaderi, D., Verma, I. M., Liu, Y. T., Messer, K., Chen, X., Varki, A., and Schwab, R. (2011) Human xeno-autoantibodies against a non-human sialic acid serve as novel serum biomarkers and immunotherapeutics in cancer. *Cancer Res.* **71**, 3352–3363
 33. Willett, W. C. (2000) Diet and cancer. *Oncologist* **5**, 393–404
 34. Norat, T., Lukanova, A., Ferrari, P., and Riboli, E. (2002) Meat consumption and colorectal cancer risk. Dose-response meta-analysis of epidemiological studies. *Int. J. Cancer* **98**, 241–256
 35. Zhang, J., and Kesteloot, H. (2005) Milk consumption in relation to incidence of prostate, breast, colon, and rectal cancers. Is there an independent effect? *Nutr. Cancer* **53**, 65–72
 36. Wiseman, M. (2008) The second World Cancer Research Fund/American Institute for Cancer Research expert report. Food, nutrition, physical activity, and the prevention of cancer. A global perspective. *Proc. Nutr. Soc.* **67**, 253–256
 37. Pham, T., Gregg, C. J., Karp, F., Chow, R., Padler-Karavani, V., Cao, H., Chen, X., Witztum, J. L., Varki, N. M., and Varki, A. (2009) Evidence for a novel human-specific xeno-auto-antibody response against vascular endothelium. *Blood* **114**, 5225–5235
 38. Hedlund, M., Padler-Karavani, V., Varki, N. M., and Varki, A. (2008) Evidence for a human-specific mechanism for diet and antibody-mediated inflammation in carcinoma progression. *Proc. Natl. Acad. Sci. U.S.A.* **105**, 18936–18941
 39. Kean, E. L., and Roseman, S. (1966) The sialic acids. X. Purification and properties of cytidine 5'-monophosphosialic acid synthetase. *J. Biol. Chem.* **241**, 5643–5650
 40. Higa, H. H., and Paulson, J. C. (1985) Sialylation of glycoprotein oligosaccharides with *N*-acetyl-, *N*-glycolyl-, and *N*-*O*-diacetylneuraminic acids. *J. Biol. Chem.* **260**, 8838–8849
 41. Bulai, T., Bratosin, D., Artenie, V., and Montreuil, J. (2002) Characterization of a sialate pyruvate-lyase in the cytosol of human erythrocytes. *Biochimie* **84**, 655–660
 42. Schauer, R., Sommer, U., Krüger, D., van Unen, H., and Traving, C. (1999) The terminal enzymes of sialic acid metabolism. Acylneuraminase pyruvate-lyases. *Biosci. Rep.* **19**, 373–383
 43. Yamada-Okabe, T., Sakamori, Y., Mio, T., and Yamada-Okabe, H. (2001) Identification and characterization of the genes for *N*-acetylglucosamine kinase and *N*-acetylglucosamine-phosphate deacetylase in the pathogenic fungus *Candida albicans*. *Eur. J. Biochem.* **268**, 2498–2505
 44. Weihofen, W. A., Berger, M., Chen, H., Saenger, W., and Hinderlich, S. (2006) Structures of human *N*-acetylglucosamine kinase in two complexes with *N*-acetylglucosamine and with ADP/glucose. Insights into substrate specificity and regulation. *J. Mol. Biol.* **364**, 388–399
 45. Hall, R. S., Xiang, D. F., Xu, C., and Rauschel, F. M. (2007) *N*-Acetyl-D-glucosamine-6-phosphate deacetylase. Substrate activation via a single divalent metal ion. *Biochemistry* **46**, 7942–7952
 46. Bergfeld, A. K., Claus, H., Lorenzen, N. K., Spielmann, F., Vogel, U., and Mühlhoff, M. (2009) The polysialic acid-specific *O*-acetyltransferase OatC from *Neisseria meningitidis* serogroup C evolved apart from other bacterial sialate *O*-acetyltransferases. *J. Biol. Chem.* **284**, 6–16
 47. Paladini, A. C., and Leloir, L. F. (1952) Studies on uridine-diphosphate-glucose. *Biochem. J.* **51**, 426–430
 48. Trevelyan, W. E., Procter, D. P., and Harrison, J. S. (1950) Detection of sugars on paper chromatograms. *Nature* **166**, 444–445
 49. Wazer, D. E., Liu, X. L., Chu, Q., Gao, Q., and Band, V. (1995) Immortalization of distinct human mammary epithelial cell types by human papilloma virus 16 E6 or E7. *Proc. Natl. Acad. Sci. U.S.A.* **92**, 3687–3691
 50. Choo, A., Padmanabhan, J., Chin, A., Fong, W. J., and Oh, S. K. (2006) Immortalized feeders for the scale-up of human embryonic stem cells in feeder and feeder-free conditions. *J. Biotechnol.* **122**, 130–141
 51. Auwerx, J. (1991) The human leukemia cell line, THP-1. A multifaceted model for the study of monocyte-macrophage differentiation. *Experientia* **47**, 22–31
 52. Sjöberg, E. R., Manzi, A. E., Khoo, K. H., Dell, A., and Varki, A. (1992) Structural and immunological characterization of *O*-acetylated GD2. Evidence that GD2 is an acceptor for ganglioside *O*-acetyltransferase in human melanoma cells. *J. Biol. Chem.* **267**, 16200–16211
 53. Menezes, J., Leibold, W., Klein, G., and Clements, G. (1975) Establishment and characterization of an Epstein-Barr virus (EBV)-negative lymphoblastoid B cell line (BJA-B) from an exceptional, EBV-genome-negative Afri-

- can Burkitt's lymphoma. *Biomedicine* **22**, 276–284
54. Keppler, O. T., Hinderlich, S., Langner, J., Schwartz-Albiez, R., Reutter, W., and Pawlita, M. (1999) UDP-GlcNAc 2-epimerase. A regulator of cell surface sialylation. *Science* **284**, 1372–1376
 55. Pearce, O. M., and Varki, A. (2010) Chemo-enzymatic synthesis of the carbohydrate antigen N-glycolylneuraminic acid from glucose. *Carbohydr. Res.* **345**, 1225–1229
 56. Sinay, P. (1971) Synthé du 3-O-(D-1-carboxyéthyl)-2-désoxy-2-glycol-amido-D-glucose (acide N-glycolylmuramique). *Carbohydr. Res.* **16**, 113–122
 57. Sampathkumar, S. G., Li, A. V., Jones, M. B., Sun, Z., and Yarema, K. J. (2006) Metabolic installation of thiols into sialic acid modulates adhesion and stem cell biology. *Nat. Chem. Biol.* **2**, 149–152
 58. Jourdian, G. W., and Roseman, S. (1962) The sialic acids. II. Preparation of N-glycolylhexosamines, N-glycolylhexosamine 6-phosphates, glycolyl coenzyme A, and glycolyl glutathione. *J. Biol. Chem.* **237**, 2442–2446
 59. Nöhle, U., Beau, J. M., and Schauer, R. (1982) Uptake, metabolism, and excretion of orally and intravenously administered, double-labeled N-glycolylneuraminic acid and single-labeled 2-deoxy-2,3-dehydro-N-acetylneuraminic acid in mouse and rat. *Eur. J. Biochem.* **126**, 543–548
 60. Li, Y., Yu, H., Cao, H., Lau, K., Muthana, S., Tiwari, V. K., Son, B., and Chen, X. (2008) *Pasteurella multocida* sialic acid aldolase. A promising biocatalyst. *Appl. Microbiol. Biotechnol.* **79**, 963–970
 61. Kent, P. W., and Allen, A. (1968) The biosynthesis of intestinal mucins. The effect of salicylate on glycoprotein biosynthesis by sheep colonic and human gastric mucosal tissues *in vitro*. *Biochem. J.* **106**, 645–658
 62. Vamecq, J., Mestdagh, N., Henichart, J. P., and Poupaert, J. (1992) Subcellular distribution of glycolyltransferases in rodent liver and their significance in special reference to the synthesis of N-glycolylneuraminic acid. *J. Biochem.* **111**, 579–583
 63. Vamecq, J., Draye, J. P., and Poupaert, J. H. (1990) Studies on the metabolism of glycolyl-CoA. *Biochem. Cell Biol.* **68**, 846–851
 64. Koda, T., Aosasa, M., Asaoka, H., Nakaba, H., and Matsuda, H. (2003) Application of tyramide signal amplification for detection of N-glycolylneuraminic acid in human hepatocellular carcinoma. *Int. J. Clin. Oncol.* **8**, 317–321
 65. Tse, K. P., Su, W. H., Chang, K. P., Tsang, N. M., Yu, C. J., Tang, P., See, L. C., Hsueh, C., Yang, M. L., Hao, S. P., Li, H. Y., Wang, M. H., Liao, L. P., Chen, L. C., Lin, S. R., Jorgensen, T. J., Chang, Y. S., and Shugart, Y. Y. (2009) Genome-wide association study reveals multiple nasopharyngeal carcinoma-associated loci within the HLA region at chromosome 6p21.3. *Am. J. Hum. Genet.* **85**, 194–203
 66. Takehara, A., Hosokawa, M., Eguchi, H., Ohigashi, H., Ishikawa, O., Nakamura, Y., and Nakagawa, H. (2007) γ -Aminobutyric acid (GABA) stimulates pancreatic cancer growth through overexpressing GABAA receptor π subunit. *Cancer Res.* **67**, 9704–9712
 67. Watanabe, M., Maemura, K., Oki, K., Shiraishi, N., Shibayama, Y., and Katsu, K. (2006) γ -Aminobutyric acid (GABA) and cell proliferation. Focus on cancer cells. *Histol. Histopathol.* **21**, 1135–1141
 68. Matuszek, M., Jesipowicz, M., and Kleinrok, Z. (2001) GABA content and GAD activity in gastric cancer. *Med. Sci. Monit.* **7**, 377–381
 69. Inoue, S., Sato, C., and Kitajima, K. (2010) Extensive enrichment of N-glycolylneuraminic acid in extracellular sialoglycoproteins abundantly synthesized and secreted by human cancer cells. *Glycobiology* **20**, 752–762
 70. Schauer, R., and Wember, M. (1996) Isolation and characterization of sialate lyase from pig kidney. *Biol. Chem. Hoppe-Seyler* **377**, 293–299
 71. Sommer, U., Traving, C., and Schauer, R. (1999) The sialate pyruvate-lyase from pig kidney. Purification, properties, and genetic relationship. *Glycoconj. J.* **16**, 425–435
 72. Brunetti, P., Jourdian, G. W., and Roseman, S. (1962) The sialic acids. III. Distribution and properties of animal N-acetylneuraminic aldolase. *J. Biol. Chem.* **237**, 2447–2453
 73. Ghosh, S., and Roseman, S. (1965) The sialic acids. V. N-Acyl-D-glucosamine 2-epimerase. *J. Biol. Chem.* **240**, 1531–1536
 74. Luchansky, S. J., Yarema, K. J., Takahashi, S., and Bertozzi, C. R. (2003) GlcNAc 2-epimerase can serve a catabolic role in sialic acid metabolism. *J. Biol. Chem.* **278**, 8035–8042
 75. Hinderlich, S., Berger, M., Schwarzkopf, M., Effertz, K., and Reutter, W. (2000) Molecular cloning and characterization of murine and human N-acetylglucosamine kinase. *Eur. J. Biochem.* **267**, 3301–3308
 76. Weidanz, J. A., Campbell, P., Moore, D., DeLucas, L. J., Rodén, L., Thompson, J. N., and Vezza, A. C. (1996) N-Acetylglucosamine kinase and N-acetylglucosamine-6-phosphate deacetylase in normal human erythrocytes and *Plasmodium falciparum*. *Br. J. Haematol.* **95**, 645–653
 77. Campbell, P., Laurent, T. C., and Rodén, L. (1987) Assay and properties of N-acetylglucosamine-6-phosphate deacetylase from rat liver. *Anal. Biochem.* **166**, 134–141
 78. Fujita, A., Sato, C., and Kitajima, K. (2007) Identification of the nuclear export signals that regulate the intracellular localization of the mouse CMP-sialic acid synthetase. *Biochem. Biophys. Res. Commun.* **355**, 174–180
 79. Münster-Kühnel, A. K., Tiralongo, J., Krapp, S., Weinhold, B., Ritz-Sedlacek, V., Jacob, U., and Gerardy-Schahn, R. (2004) Structure and function of vertebrate CMP-sialic acid synthetases. *Glycobiology* **14**, 43R–51R
 80. Collins, B. E., Fralich, T. J., Itonori, S., Ichikawa, Y., and Schnaar, R. L. (2000) Conversion of cellular sialic acid expression from N-acetyl- to N-glycolylneuraminic acid using a synthetic precursor, N-glycolylmannosamine pentaacetate. Inhibition of myelin-associated glycoprotein binding to neural cells. *Glycobiology* **10**, 11–20
 81. Sarkar, A. K., Fritz, T. A., Taylor, W. H., and Esko, J. D. (1995) Disaccharide uptake and priming in animal cells. Inhibition of sialyl Lewis X by acetylated Gal β 1 \rightarrow 4GlcNAc β -O-naphthalenemethanol. *Proc. Natl. Acad. Sci. U.S.A.* **92**, 3323–3327
 82. Varki, A. (2009) Multiple changes in sialic acid biology during human evolution. *Glycoconj. J.* **26**, 231–245
 83. Dharmawardhane, S., Schürmann, A., Sells, M. A., Chernoff, J., Schmid, S. L., and Bokoch, G. M. (2000) Regulation of macropinocytosis by p21-activated kinase-1. *Mol. Biol. Cell* **11**, 3341–3352
 84. Johannes, L., and Lamaze, C. (2002) Clathrin-dependent or not. Is it still the question? *Traffic* **3**, 443–451
 85. Simonsen, A., Wurmser, A. E., Emr, S. D., and Stenmark, H. (2001) The role of phosphoinositides in membrane transport. *Curr. Opin. Cell Biol.* **13**, 485–492
 86. Yin, J., Hashimoto, A., Izawa, M., Miyazaki, K., Chen, G. Y., Takematsu, H., Kozutsumi, Y., Suzuki, A., Furuhashi, K., Cheng, F. L., Lin, C. H., Sato, C., Kitajima, K., and Kannagi, R. (2006) Hypoxic culture induces expression of sialin, a sialic acid transporter, and cancer-associated gangliosides containing non-human sialic acid on human cancer cells. *Cancer Res.* **66**, 2937–2945
 87. Ghaderi, D., Taylor, R. E., Padler-Karavani, V., Diaz, S., and Varki, A. (2010) Implications of the presence of N-glycolylneuraminic acid in recombinant therapeutic glycoproteins. *Nat. Biotechnol.* **28**, 863–867
 88. Macauley, M. S., Chan, J., Zandberg, W., He, Y., Whitworth, G. A., Stubbs, K. A., Yuzwa, S., Varki, A., Davies, G. J., and Vocadlo, D. J. (2012) Metabolism of vertebrate amino sugars with N-glycolyl groups. Resistance of α 2-8-linked N-glycolylneuraminic acid to enzymatic cleavage. *J. Biol. Chem.* **287**, 28917–28931
 89. Bergfeld, A. K., Pearce, O. M., Diaz, S. L., Lawrence, R., Vocadlo, D. J., Choudhury, B., Esko, J. D., and Varki, A. (2012) Metabolism of vertebrate amino sugars with N-glycolyl groups. Incorporation of N-glycolylhexosamines into mammalian glycans by feeding N-glycolylgalactosamine. *J. Biol. Chem.* **287**, 28898–28916
 90. Takahashi, S., Takahashi, K., Kaneko, T., Ogasawara, H., Shindo, S., and Kobayashi, M. (1999) Human renin-binding protein is the enzyme N-acetyl-D-glucosamine 2-epimerase. *J. Biochem.* **125**, 348–353

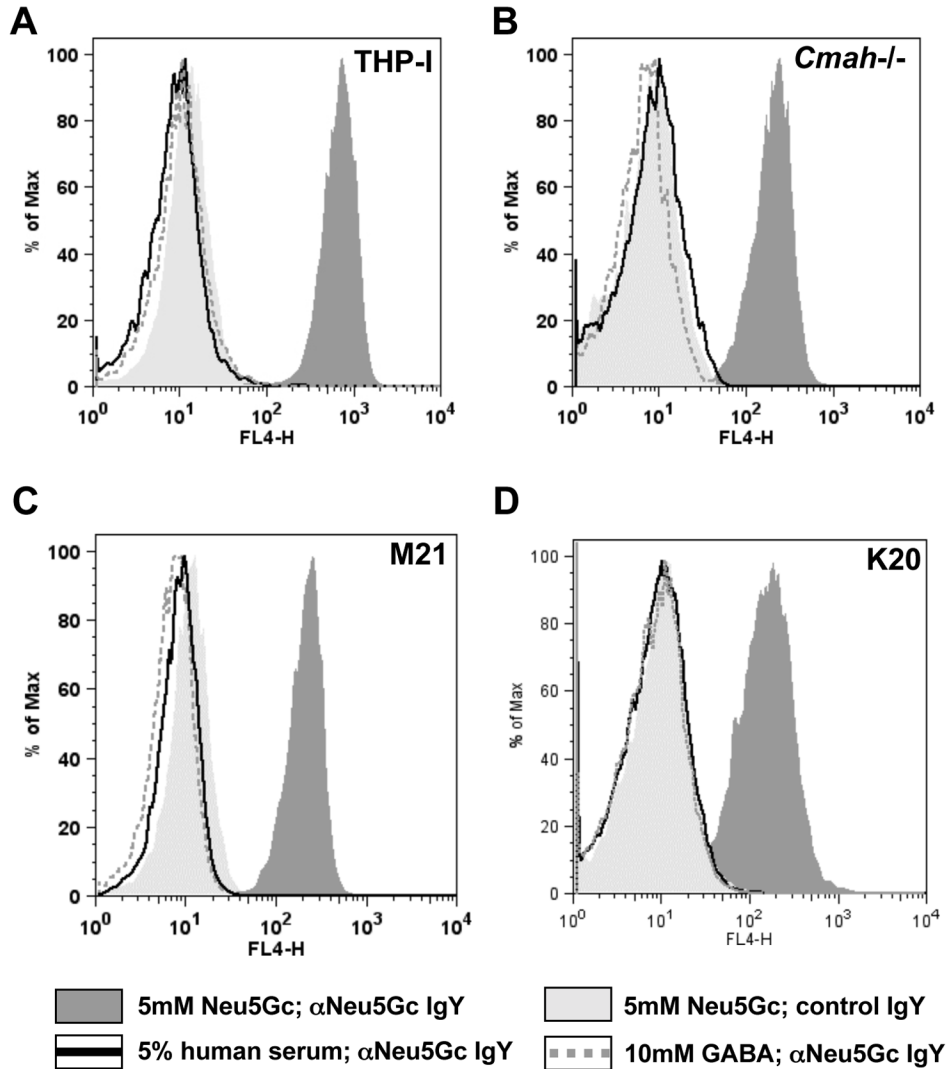


FIGURE S1: Various human cell lines were shown to be devoid of Neu5Gc *de novo* biosynthesis. Murine *Cmah*^{-/-} fibroblasts, human THP-I cells, human melanoma cell line M21 as well as human B-cell lymphoma cell line BJAB-K20 were cultivated under Neu5Gc-free conditions using 5% human serum. The feeding media were supplemented with either 5mM Neu5Gc (positive control; shaded dark grey) or 10mM γ -Aminobutyric acid (GABA; dotted grey line). In parallel, cells were kept in 5% human serum with no additional supplements (negative control; black line). After 3 days incubation, cells were harvested and analyzed by flow cytometry using the polyclonal chicken anti-Neu5Gc antibody (α Neu5Gc IgY; {Diaz *et al.*, 2009, #65670}) to sensitively detect cell-surface glycosidically-bound Neu5Gc. As an additional negative control, cells fed with 5mM Neu5Gc were also stained with control chicken IgY antibody (control IgY, shaded light grey). **A**, THP-I cells. **B**, *Cmah*^{-/-} fibroblasts. **C**, M21-cells. **D**, BJA-B K20 cells.

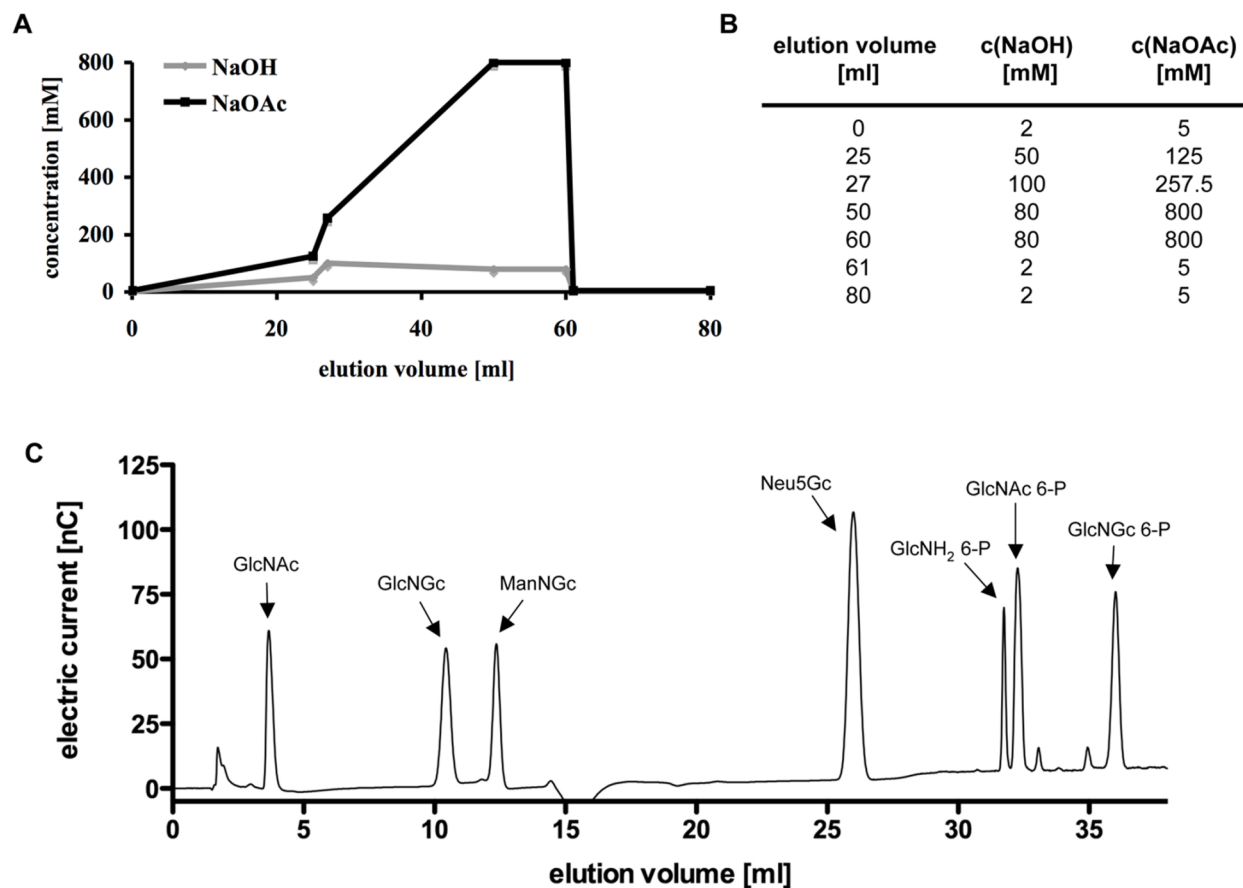


FIGURE S2: **HPAEC-PAD HPLC analyses.** **A**, Profile of the gradient used to separate N-glycolylhexosamine intermediates of the proposed degradative pathway by HPLC using a PA-1 column under alkaline conditions. The gradient is composed of several individual linear gradients and the concentration of sodium hydroxide (NaOH, grey line) and sodium acetate (NaOAc, black line) is depicted for the whole gradient. The flow rate was set to 1ml/min. **B**, summary mentioning exact concentrations of NaOH and NaOAc at the start- and end-points of all linear gradients involved in the method. **C**, elution profile of PA-1 column using the gradient described above. Loaded compounds include synthesized Neu5Gc, ManNGc, GlcNGc, and GlcNGc 6-P as well as commercial GlcNAc, GlcNAc 6-P, and GlcNH₂ 6-P.

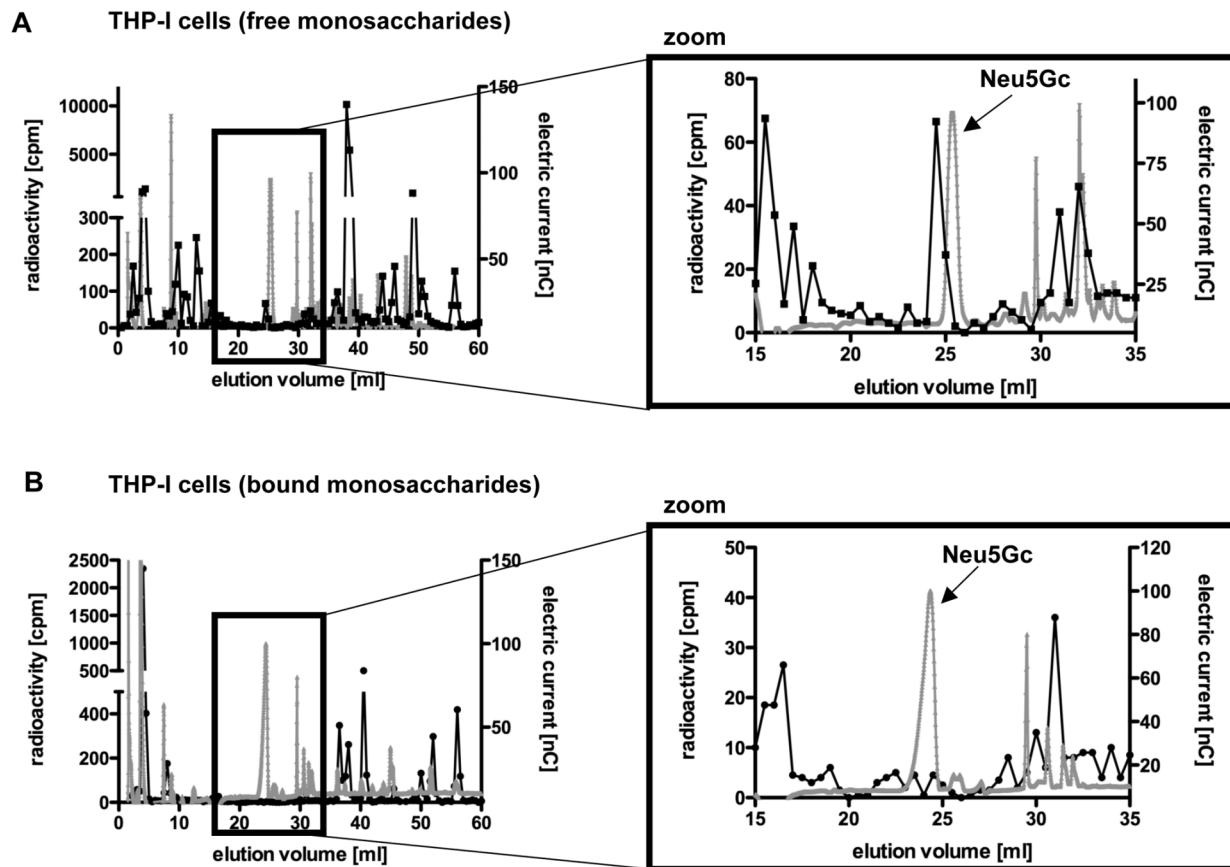


FIGURE S3. THP-I cells incorporate ^3H glycolic acid into multiple structures but do not use it as a precursor for Neu5Gc synthesis. Human THP-I cells were cultivated under Neu5Gc-free conditions using 5% human serum and thereafter the feeding medium was supplemented with synthesized ^3H glycolic acid. After 3 days, the feeding medium was removed, and the cells were washed with PBS. Subsequently, the cell pellets were resuspended in hypotonic 10mM TrisHCl (pH 7.5) and lysed by repetitive freeze-thaw. Ethanol was added to a final concentration of 70% and precipitation occurred overnight at -20°C . The supernatant of the Ethanol precipitation contains the free monosaccharides and was dried down. The pellet contains the bound monosaccharides and was therefore treated with sialidase to release potential sialic acids followed by an additional Ethanol precipitation. This second Ethanol supernatant was also dried down. Both samples were then resuspended in water, supplemented with internal standards Neu5Gc, Mannose, and ^3H Mannose and analyzed by HPLC under alkaline conditions using a PA-1 column using HPAEC-PAD. Also fractions (0.5ml) were collected and radioactivity determined by scintillation counting. Radioactivity is depicted in cpm (left Y-axis; black symbols and line) and electric current is represented in nC (right Y-axis; grey symbols and line). The exact overlay of the two spectra was confirmed by cold and radiolabeled mannose standards. The complete chromatograms are shown (left panel) and a zoomed portion (right panel) confirms the absence of a significant peak in the radioactive spectra overlaying with the internal standard Neu5Gc detected by HPAEC-PAD. **A**, free monosaccharides and **B**, sialidase-released bound monosaccharides.

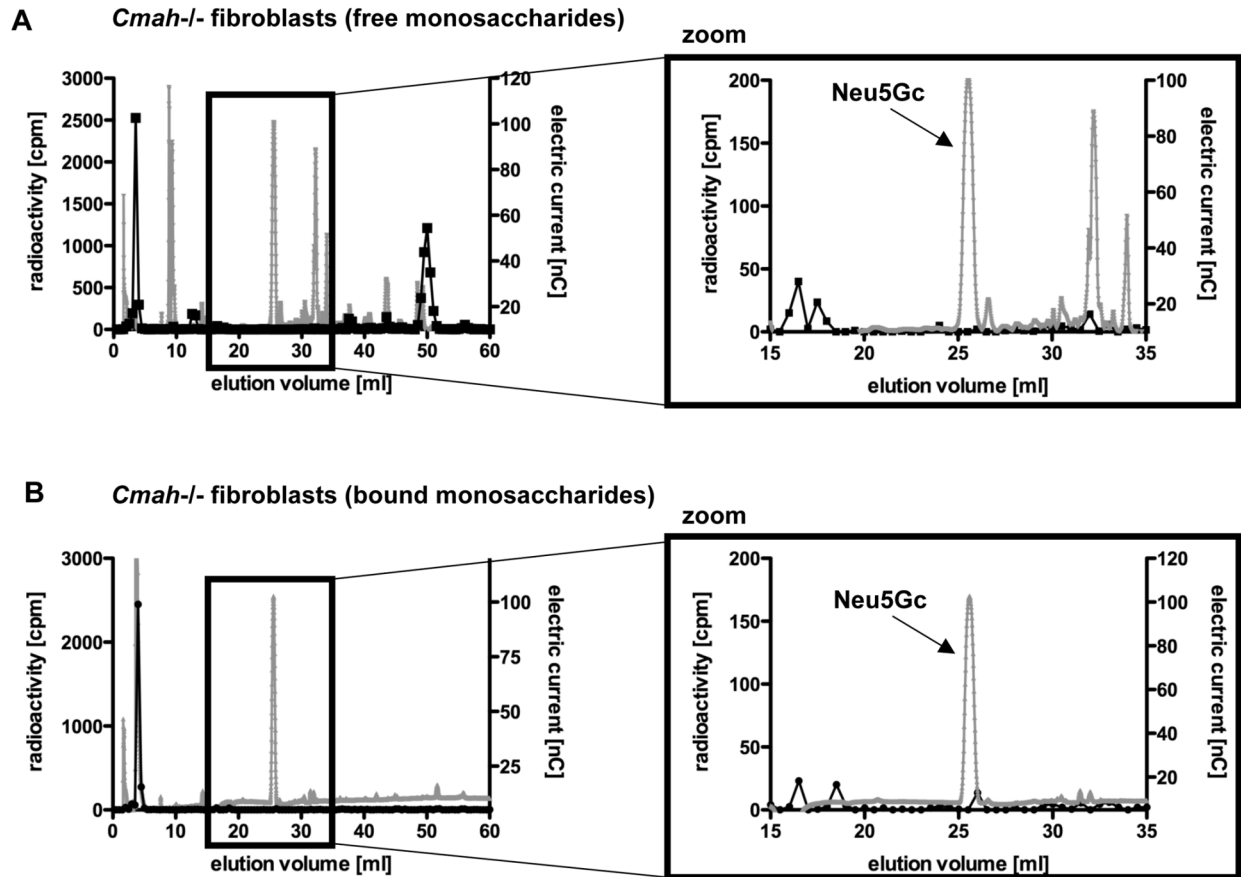


FIGURE S4. *Cmah*^{-/-} fibroblasts are not capable to synthesize Neu5Gc in the presence of [³H]glycolic acid. Neu5Gc-deficient *Cmah*^{-/-} fibroblasts were cultivated under Neu5Gc-free conditions using 5% human serum and thereafter the feeding medium was supplemented with synthesized [³H]glycolic acid. After 3 days, the feeding medium was removed, and the cells were washed intensively with PBS. Subsequently, the cell pellets were resuspended in hypotonic 10mM TrisHCl (pH 7.5) and lysed by repetitive freeze-thaw. Ethanol was added to a final concentration of 70% and precipitation occurred overnight at -20°C. **A**, the supernatant containing free monosaccharides was decanted for analysis and **B**, the pellet was washed well, resolved, and treated with sialidase to release sialic acids from sialoglycoconjugates. Liberated monosaccharides were then cleaned up by an additional Ethanol precipitation to remove proteins and membrane debris and the resulting supernatant containing the potential released Sias, was also analyzed. Samples were dried down, reconstituted in water, and spiked with Neu5Gc, Mannose and [³H]Mannose as internal standards. Monosaccharide composition was analyzed by HPLC using a PA-1 column under alkaline conditions. In parallel to HPAEC-PAD, fractions (0.5ml) were collected and radioactivity was subsequently measured by scintillation counting. Radioactivity is depicted in cpm (left Y-axis; black symbols and line) and electric current is represented in nC (right Y-axis; grey symbols and line). The exact overlay of the two spectra was confirmed by cold and radiolabeled mannose standards. The complete chromatograms are shown (left panel) and a zoomed portion (right panel) confirms the absence of a significant peak in the radioactive spectra overlaying with the internal standard Neu5Gc detected by HPAEC-PAD.

Primer name		Sequence (5'-3')
AKB 3	s	GGAGTCATATGATGCGCGGCGAGCAGGGCGC
AKB 9	as	CCGTCCTCGAGCTGCCTAGCTGCGTCCGCC
AKB 11	s	CTAGAAAGAAGGAGACGGACATATGGCTAGCG
AKB 12	as	GATCCGCTAGCCATATGTCCGTCTCCTTCTTT
AKB 20	s	GGTAGGAATTCGCATGGCCGCGATCTATGGGG
AKB 21	as	GTGGTCTCGAGCTAGGAAAAGGTGTAGGAATAG

FIGURE S5. **Oligonucleotides used in the current study.** The sequences of all sense (s) and antisense (as) primers used in this study are listed in 5'-3' direction.